*Shimakami, T. et al.：Proc. Natl. Acad. Sci. USA, 109：941-946, 2012*

# miR-122－Ago2複合体による C型肝炎ウイルスRNAの安定化

島上哲朗，山根大典，Stanley M. Lemon

肝臓特異的なマイクロRNAであるmiR-122は，C型肝炎ウイルス（HCV）の複製を促進することが知られていたが，その分子機構は不明であった．今回われわれは，miR-122がHCV RNAの5′末端に結合することでHCV RNAを安定化すること，さらにその安定化にはAgo2（Argonaute 2）が必須であることを明らかにした．

C型肝炎ウイルス（HCV）は，約9.6 kbの一本鎖＋鎖RNAウイルスで，C型慢性肝炎，肝硬変，肝がんの原因である．一方miR-122は，肝臓特異的なmiRNA（マイクロRNA）であり，肝臓内miRNAの約60％を占めている．Sarnowらのグループは，HCVの5′非翻訳領域（UTR）にmiR-122結合部位が2カ所存在し，miR-122は*HCV* 5′UTRとの結合を介してHCV複製を促進することを報告した（図1 A）[1)～3)]．またLanfordらは，HCV感染チンパンジーにmiR-122を阻害するアンチセンス鎖を投与し，その強力な抗ウイルス効果を報告した[4)]．そのためmiR-122は抗HCV薬の有力な標的として注目されている．一般にmiRNAは，細胞mRNAの3′UTR領域に結合し標的タンパク質発現を抑制するため，miR-122によるHCV複製の促進はmiRNAの機能としてはきわめてユニークなものである．その後miR-122はHCVのIRES（internal ribosome entry site）依存性のタンパク質翻訳を促進することが報告されたが[5)]，その詳細な分子機構は不明であった．今回われわれはmiR-122がHCV RNAを安定化することでタンパク質発現を促進し，その安定化にAgo2（Argonaute 2）が必須であることを明らかにした．

## miR-122は細胞内に導入したHCV RNAを安定化することでタンパク質発現を促進する

まずわれわれは，miR-122のHCV RNAへの安定性とタンパク質発現に対する影響とを同時に検討するため，HCVのp7（ウイルス粒子の構造タンパク質の1つ）と非構造タンパク質NS2との間にGLuc（*Gaussia* luciferase）と口蹄疫ウイルスの2A配列（FMDV2A）を挿入した．GLucはFMDV2Aの自己プロテアーゼ活性による切断を受け，自身の分泌シグナル依存的に細胞外へ分泌されることから，細胞上清中のGLuc活性を測定することでウイルスタンパク質発現を定量した．さらにmiR-122のHCV RNA複製に対する影響を除外するため，HCVのRNA複製酵素NS5Bの活性中心GDDを不活性のAAGに置換したHCV RNAを実験に

Stabilization of hepatitis C virus RNA by an Ago2-miR-122 complex
Tetsuro Shimakami[1)]/Daisuke Yamane[2)]/Stanley M. Lemon[2)]：Department of Disease Control and Homeostasis, Division of Environmental Science, Kanazawa University Graduate School of Medical Science[1)]/Lineberger Comprehensive Cancer Center and Division of Infectious Diseases, Department of Medicine, University of North Carolina at Chapel Hill[2)]（金沢大学大学院医学系研究科環境医科学専攻恒常性制御学講座[1)]/ノースカロライナ大学チャペルヒル校医学部ラインバーガー総合がんセンター[2)]）

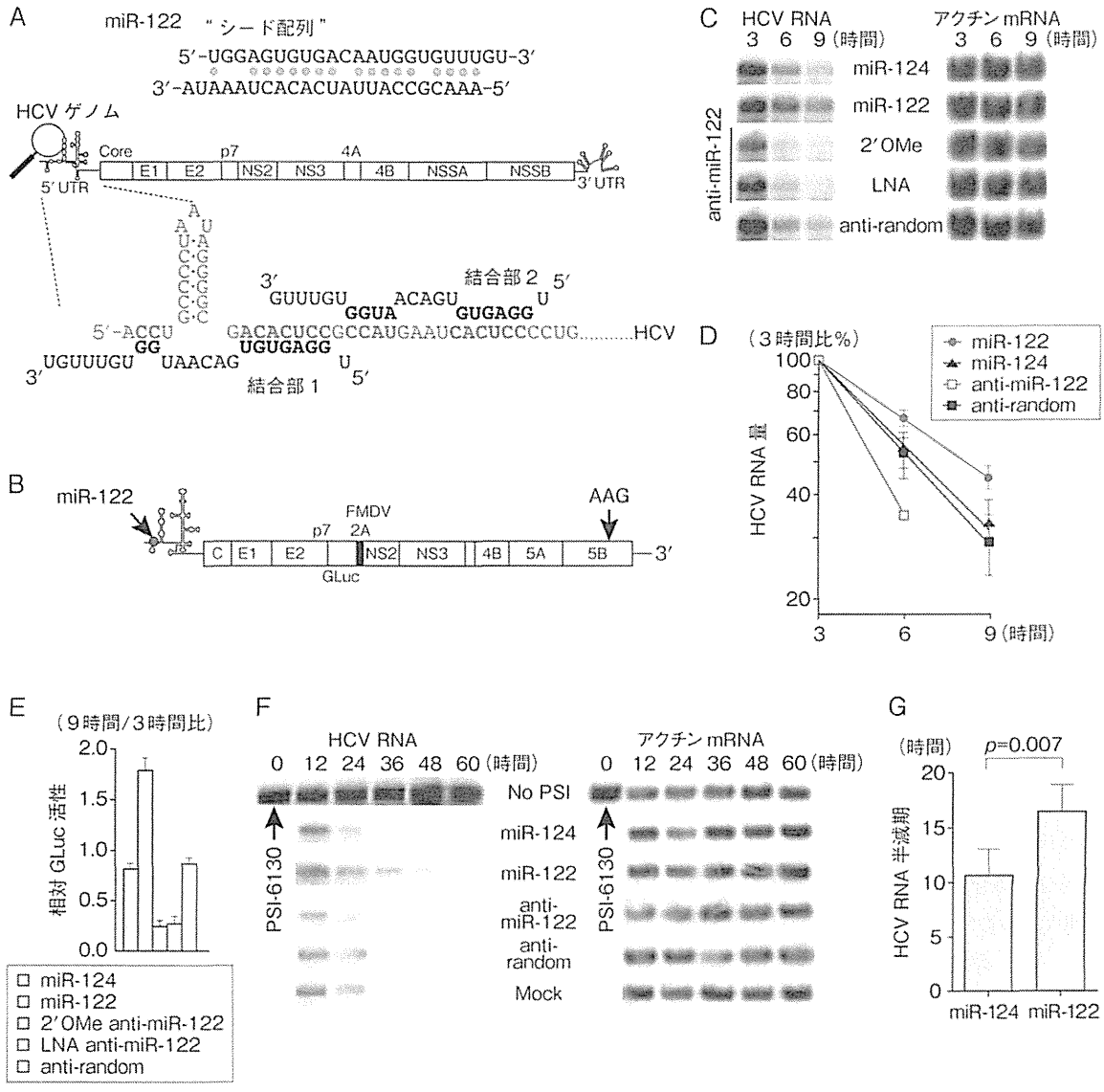


図1　miR-122は，HCV RNAを安定化する

A) HCVゲノムとmiR-122．HCVは5′UTRに2カ所のmiR-122結合部位を有する．B) GLucを含んだ非複製HCV RNA，H77S/GLuc2A/AAG．p7とNS2の間にGLuc，FMDV2A配列を挿入し，NS5Bの活性中心GDDを不活性のAAGに置換した．C) miR-122およびアンチセンス鎖（anti-miR-122）のHCV RNAの安定性に対する影響．H77S/GLuc2A/AAGを図に示すmiRNAまたは一本鎖RNAとともにエレクトロポレーションにより細胞内導入し，3時間おきに細胞トータルRNAを回収した後，HCV RNAとアクチンmRNAをノーザンブロット法により定量した．D) miR-122のHCV RNAの安定性に対する影響．Cの結果を定量し，3時間値に対するHCV RNAの減衰を示す．E) miR-122のHCV RNAのタンパク質翻訳に対する影響．H77S/GLuc2A/AAGを，図に示すmiRNAまたは一本鎖RNAとともに細胞内導入し，3時間おきに細胞上清を回収後GLuc活性を測定し，9時間値を3時間値で補正した．F) miR-122の持続感染細胞内HCV RNAの安定性に対する影響．HCV持続感染細胞にNS5B阻害剤PSI-6130を投与し，RNA複製を抑制した状態で，図に示すmiRNAまたは一本鎖RNAを導入し，細胞トータルRNAを12時間おきに回収した後，HCV RNAとアクチンmRNAをノーザンブロット法により定量した．G) HCV持続感染細胞におけるmiR-122によるHCV RNA半減期の延長．Fを定量し，算出した（文献6より転載）

用いた（H77S/GLuc2A/AAG，図1B）．この複製能を有しないHCV RNAをmiR-122あるいは2種類のmiR-122に対するアンチセンス鎖（anti-miR-122，2′O-methyl：2′OMe，locked nucleic acid：LNA修飾）とともに肝がん細胞株Huh-7細胞にエレクトロポレーションにより導入し，細胞トータルRNAと細胞上清の回収を3時間間隔で9時間後まで行った．脳特異的なmiRNAであるmiR-124と，いずれのmiRNAとも結合しない一本鎖RNA（anti-random）をコントロールとして用いた．HCV RNAの安定性に関しては，HCVに対するプローブを用いてノーザンブロット解析により評価した．図1C，Dに示すようにmiR-122はmiR-124に比べてHCV RNAを安定化し，逆にanti-miR-122はanti-randomに比べてHCV RNAを不安定化した．同時に細胞上清中のGLuc活性を測定したところ，miR-122とanti-miR-122のGLuc活性への影響はHCV RNAの安定性に対する影響とほぼ同一であった（図1E）．これらの結果からmiR-122はHCV RNAの安定性を増加させることでHCVタンパク質発現を促進していることが明らかとなった．

## miR-122はHCV持続感染細胞においてもHCV RNAを安定化する

前述の結果は，非複製HCV RNAを用いている点，また大量の合成HCV RNAを細胞内に導入している点で非生理的である．細胞内で持続的に複製しているHCV RNAと非複製HCV RNAの分解経路は異なる可能性が考えられたことから，HCV持続感染細胞を作成し，複製HCV RNAに対するmiR-122の影響を検討した．miR-122のHCV RNA合成に対する影響を除外するため，NS5B特異的阻害剤PSI-6130を半有効濃度の約10倍量でHCV持続感染細胞に投与し，HCV RNA合成を停止させた．同時にmiR-122，anti-miR-122およびコントロールを投与し，12時間間隔で60時間後まで細胞トータルRNAを回収し，ノーザンブロット解析によってHCV RNAの安定性を評価した（図1F：ノーザンブロット，G：HCV RNA半減期）．その結果HCV感染細胞においてもmiR-122は有意にHCV RNAを安定化し半減期を延長することが明らかとなった．

## miR-122はAgo2とともにHCV RNAとの複合体を形成する

一般にsiRNAやmiRNAなどのスモールRNAは，それ自身が単独で働くのではなく，RNA誘導サイレンシング複合体（RISC）と複合体を形成することにより，はじめて標的遺伝子の発現を制御する．そこでまずHCV持続感染細胞を用い，RISCの主要コンポーネントであるAgo1-4がHCV複製に与える影響を検討した．siRNAを用いて，Ago1-4およびmiRNAの生合成に関与するDicerをそれぞれノックダウンし，HCV RNA量を定量RT-PCRを用いて測定したところ（図2A），Ago2ノックダウンのみにおいて HCV複製が抑制された．このことから，Ago2がmiR-122を介してHCV RNAと複合体を形成している可能性を免疫沈降法により検証した．miR-122をもたないマウス胎仔線維芽細胞（MEF）にHCV RNAとmiR-122をエレクトロポレーションにより導入し，導入後6時間のライセート中のAgo2を特異的抗体により免疫沈降し，Ago2複合体中のHCV RNAの有無をRT-PCR法にて検出した．また，配列特異的な相互作用の有無を検討するため，HCV 5′UTRの2カ所のmiR-122結合部位に点変異をもちmiR-122と結合しないHCV RNA（p6m）と，p6mとの結合能を有する変異体miR-122（miR-122p6）を作成した．コントロールIgGを用いて免疫沈降した際は，HCV RNAは検出されなかったが（図2B左），Ago2抗体を用いた際はHCV RNAとmiR-122の結合特異的なHCV RNAの存在が認められた（図2B右）．以上の結果から，Ago2はmiR-122を介してHCV RNAと複合体を形成することが明らかとなった．

## HCV RNAの安定化にはAgo2が必須である

次にmiR-122のHCV安定化機能に対するAgo2の役割をAgo2ノックアウトマウス由来MEFを用いて検討した．H77S/GLuc2A/AAG RNAをmiR-122あるいはmiR-124とともにAgo2ノックアウトおよび野生型MEFにエレクトロポレーションにて導入し，細胞トータルRNAと細胞上清の回収を3時間間隔で行い，それぞれノーザンブロットおよびGLuc活性の測定を行なった．miR-122は野生型MEFではHCV RNAを安定化したが（図2C上段），Ago2ノックアウトMEF

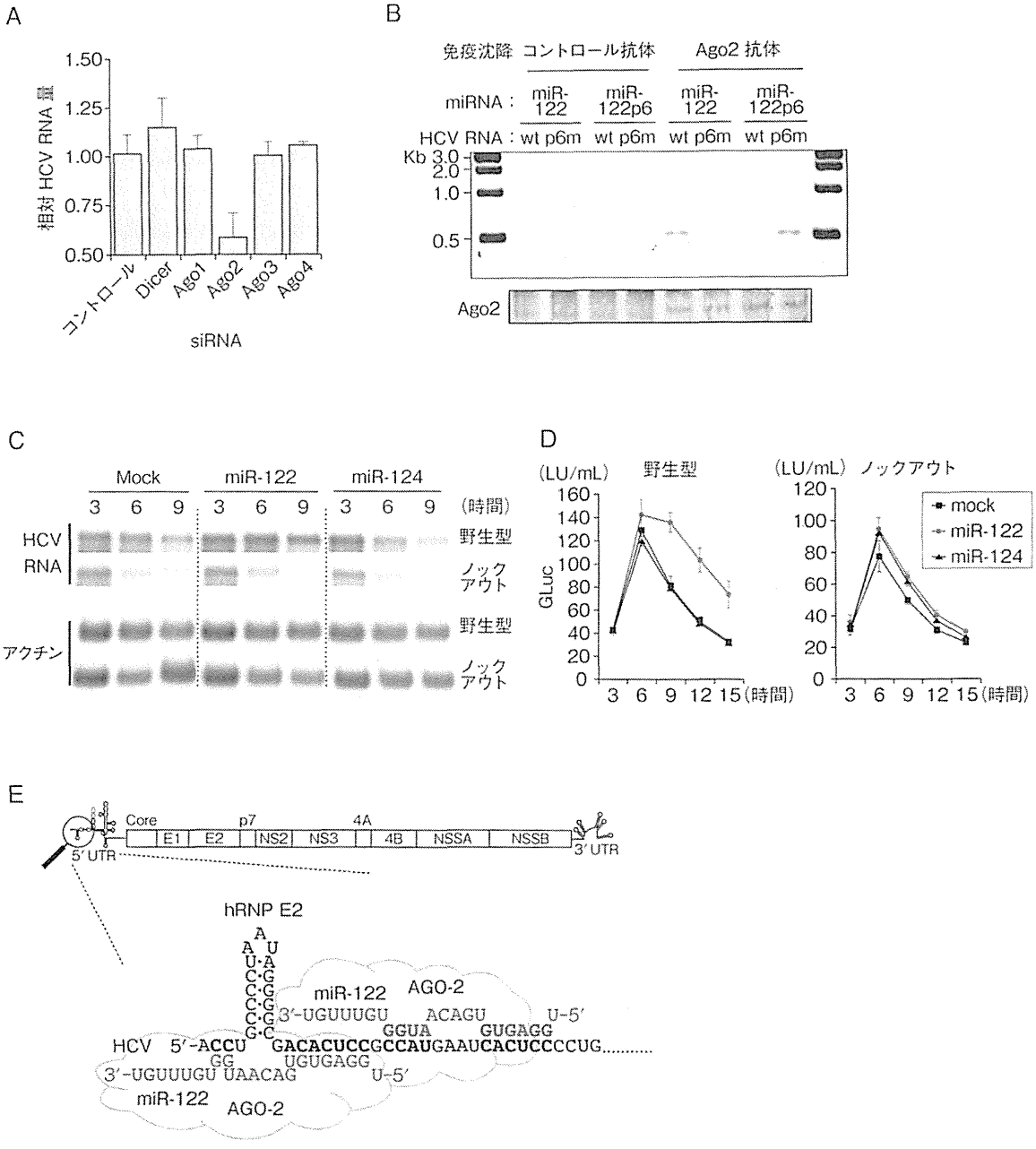


図2 miR-122によるHCV RNAの安定化にはAgo2が必須である

A) HCV複製に対するRNA誘導サイレンシング複合体（RISC）関連タンパク質の影響．HCV持続感染細胞に図に示すsiRNAを導入し，HCV複製に対する影響を定量RT-PCRを用いて評価した．B) miR-122を介したHCV RNAとAgo2との複合体形成．マウス胎仔線維芽細胞（MEF）にmiR-122とHCV RNAを導入し，特異的モノクローナル抗体を用いてAgo2を免疫沈降後，HCV RNAの有無をRT-PCR法にて検出した．p6mは，HCV RNAの5′UTRに存在する2カ所のmiR-122結合部位に結合能を欠損させる点変異を含んだ変異体で，miR-122p6は，p6mとの結合能を有する変異型miR-122．C) Ago2のmiR-122によるHCV RNA安定化機能に対する役割．Ago2ノックアウトおよび野生型MEFに，図に示すmiRNAをH77S/GLuc2A/AAGとともに導入し，細胞トータルRNAを3時間おきに回収した後，HCV RNAとActin mRNAをノーザンブロット法により検出した．D) Ago2のmiR-122によるHCV RNAのタンパク質翻訳に対する影響．Ago2ノックアウトおよび野生型MEFに，図に示すmiRNAをH77S/GLuc2A/AAGとともに導入し，細胞上清を3時間おきに回収し，GLuc活性を測定した．E) miR-122とAgo2によるHCV 5′末端での複合体形成の模式図（文献6，7より転載）

ではHCV RNAを安定化しなかった（図２C下段）．同時に，タンパク質発現への影響をGLuc活性測定によって検討したところ，miR-122は野生型MEFではタンパク質発現を促進したが（図２D左），Ago2ノックアウトMEFではタンパク質発現に影響を与えなかった（図２D右）．この結果からAgo2がmiR-122によるHCV RNAの安定化のエフェクター分子であると考えられた．

## おわりに

一般にmRNAの５′末端に存在するcap構造は，mRNAを５′-エキソヌクレアーゼによる分解から保護することが知られている．HCV RNAの５′末端にcap構造を付加して保護した場合，miR-122によるHCV RNA安定化作用は認められなかった[6]．この結果は，HCV RNAの５′末端に結合したmiR-122は，Ago2や他のタンパク質（hRNP E2など）とともに複合体を形成し，５′-エキソヌクレアーゼによる分解から保護していると考えられる（図２E）．Ago2はAgo1-4タンパク質のなかで唯一標的RNAを切断する活性を有し，miRNAによる標的遺伝子抑制のキータンパク質と考えられている．今回われわれは，miR-122がHCV RNAの５′末端にAgo2を含むタンパク質複合体をリクルートすることでその半減期を延長することを明らかにしたが，Ago2が一般的に知られている機能とは逆に標的RNAを安定化する機序は不明であり，今後のさらなる検討が必要である．

## 文献


1）Jopling, C. L. et al.：hepatitis C virus RNA abundance by a liver-specific MicroRNA. Science, 309：1577-1581, 2005
2）Jopling, C. L. et al.：Position-dependent function for a tandem microRNA miR-122-binding site located in the hepatitis C virus RNA genome. Cell Host Microbe, 17：77-85, 2008
3）Machlin, E. S. et al.：Masking the 5′terminal nucleotides of the hepatitis C virus genome by an unconventional microRNA-target RNA complex. Proc. Natl. Acad. Sci. USA, 108：3193-3198, 2011
4）Lanford, R. E. et al.：Therapeutic silencing of microRNA-122 in primates with chronic hepatitis C virus infection. Science, 327：198-201, 2010
5）Henke, J. I. et al.：microRNA-122 stimulates translation of hepatitis C virus RNA. EMBO J, 27：3300-3310, 2008
6）Shimakami, T. et al.：Stabilization of hepatitis C virus RNA by an Ago2-miR-122 complex. Proc. Natl. Acad. Sci. USA, 109：941-946, 2012
7）Shimakami, T. et al.：Base-pairing between Hepatitis C Virus RNA and miR-122 3′of its Seed Sequence is Essential for Genome Stabilization and Production of Infectious Virus. J. Virol. in press（2012）



● 筆頭著者プロフィール ●

**島上哲朗**：1998年，金沢大学医学部卒業，2004年，同大学大学院医学系研究科修了，2008年から米テキサス大学（ガルベストン校），'10年より米ノースカロライナ大学（チャペルヒル校）留学，'11年４月より金沢大学付属病院恒常性制御学講座にて，患者診療，および肝炎，肝がんの基礎研究を行なっている．

JVI
Journals.ASM.org

# Base Pairing between Hepatitis C Virus RNA and MicroRNA 122 3′ of Its Seed Sequence Is Essential for Genome Stabilization and Production of Infectious Virus

**Tetsuro Shimakami,[a]* Daisuke Yamane,[a] Christoph Welsch,[a]* Lucinda Hensley,[a] Rohit K. Jangra,[b] and Stanley M. Lemon[a]**

Division of Infectious Diseases, Department of Medicine, Inflammatory Diseases Institute and Lineberger Comprehensive Cancer Center, The University of North Carolina at Chapel Hill, Chapel Hill, North Carolina, USA,[a] and Department of Microbiology, Mount Sinai School of Medicine, New York, New York, USA[b]

**MicroRNA 122 (miR-122) facilitates hepatitis C virus (HCV) replication by recruiting an RNA-induced silencing complex (RISC)-like complex containing argonaute 2 (Ago2) to the 5′ end of the HCV genome, thereby stabilizing the viral RNA. This requires base pairing between the miR-122 "seed sequence" (nucleotides [nt] 2 to 8) and two sequences near the 5′ end of the HCV RNA: S1 (nt 22 to 28) and S2 (nt 38 to 43). However, recent reports suggest that additional base pair interactions occur between HCV RNA and miR-122. We searched 606 sequences from a public database (genotypes 1 to 6) and identified two conserved, putatively single-stranded RNA segments, upstream of S1 (nt 2 and 3) and S2 (nt 30 to 34), with potential for base pairing to miR-122 (nt 15 and 16 and nt 13 to 16, respectively). Mutagenesis and genetic complementation experiments confirmed that HCV nt 2 and 3 pair with nt 15 and 16 of miR-122 bound to S1, while HCV nt 30 to 33 pair with nt 13 to 16 of miR-122 at S2. In genotype 1 and 6 HCV, nt 4 also base pairs with nt 14 of miR-122. These 3′ supplementary base pair interactions of miR-122 are functionally important and are required for Ago2 recruitment to HCV RNA by miR-122, miR-122-mediated stabilization of HCV RNA, and production of infectious virus. However, while complementary mutations at HCV nt 30 and 31 efficiently rescued the activity of a 15C,16C miR-122 mutant targeting S2, similar mutations at nt 2 and 3 failed to rescue Ago2 recruitment at S1. These data add to the current understanding of miR-122 interactions with HCV RNA but indicate that base pairing between miR-122 and the 5′ 43 nt of the HCV genome is more complex than suggested by existing models.**

Hepatitis C virus (HCV) is a positive-strand RNA virus classified in the genus *Hepacivirus* of the family *Flaviviridae*. It is strongly hepatotropic and has an unparalleled ability among RNA viruses to establish lifelong persistent infections in the majority of persons it infects (for a review, see reference 18). About 4 million Americans are persistently infected with HCV, resulting in approximately 12,000 deaths annually due to cirrhosis and liver cancer, with particularly high rates of disease among those coinfected with human immunodeficiency virus (HIV) (6). Worldwide, more than 130 million people are infected, with an estimated 350,000 HCV-related deaths each year (23). HCV is thus important from a medical and public health perspective. It is also important as an example of an RNA virus that has achieved a uniquely close evolutionary relationship with its human host, upon which its replication depends. This relationship is exemplified by the novel role played by a particular, liver-specific microRNA (miRNA), miR-122, in the HCV life cycle.

miRNAs are ~22-nucleotide (nt) RNAs that originate from lengthier transcripts and that regulate gene expression, typically posttranscriptionally, by mediating mRNA deadenylation and degradation and/or translational repression (reviewed in reference 8). This requires loading of the "guide strand" of a miRNA duplex into an argonaute (Ago) protein-containing miRNA-induced silencing complex (miRISC) and, typically, the binding of its "seed sequence" (nt 2 to 8 of the miRNA) to the 3′-untranslated region (3′UTR) of target mRNAs. miRNAs are evolutionarily conserved, and as such, they play a controlling role in cellular metabolism by regulating a majority of all genes. At present, miRBASE (http://www.mirbase.org/) lists over 1,400 distinct human miRNAs, each of which targets a number of mRNAs. Of these, miR-122 (hsa-mir-122 or MI000442) is uniquely expressed at high abundance in the adult liver, accounting for over 50% of the mature miRNAs in hepatocytes (2). miR-122 is also expressed in Huh-7 human hepatoma cells, which are widely used to propagate laboratory strains of HCV (2).

Jopling et al. (17) demonstrated that the ability of synthetic HCV RNA to replicate in transfected Huh-7 cells is dependent upon a direct interaction of miR-122 with the 5′UTR segment of the positive-strand RNA. miR-122 binds to two sites, near the 5′ end of the HCV genome (S1 and S2), at which conserved viral sequences are complementary to the seed sequence of miR-122 (nt 2 to 7) (16) (Fig. 1A). Binding of the miR-122 seed sequence to S1 and S2 promotes protein expression from transfected synthetic viral RNA and has been suggested to enhance the efficiency of translation initiated by the HCV internal ribosome entry site (IRES) (14, 15). However, a comparison of the yields of infectious virus produced by cells transfected with HCV RNA with mutations in the miR-122 binding sites versus mutations in the IRES led us to conclude that promotion of translation is insufficient to

Received 28 February 2012 Accepted 13 April 2012
Published ahead of print 24 April 2012
Address correspondence to Stanley M. Lemon, smlemon@med.unc.edu.
* Present address: Tetsuro Shimakami, Department of Gastroenterology, Kanazawa University Graduate School of Medicine, Kanazawa, Japan; Christoph Welsch, J. W. Goethe University Hospital, Department of Internal Medicine I, Frankfurt am Main, Germany.
T.S. and D.Y. contributed equally to this article.

doi:10.1128/JVI.00513-12

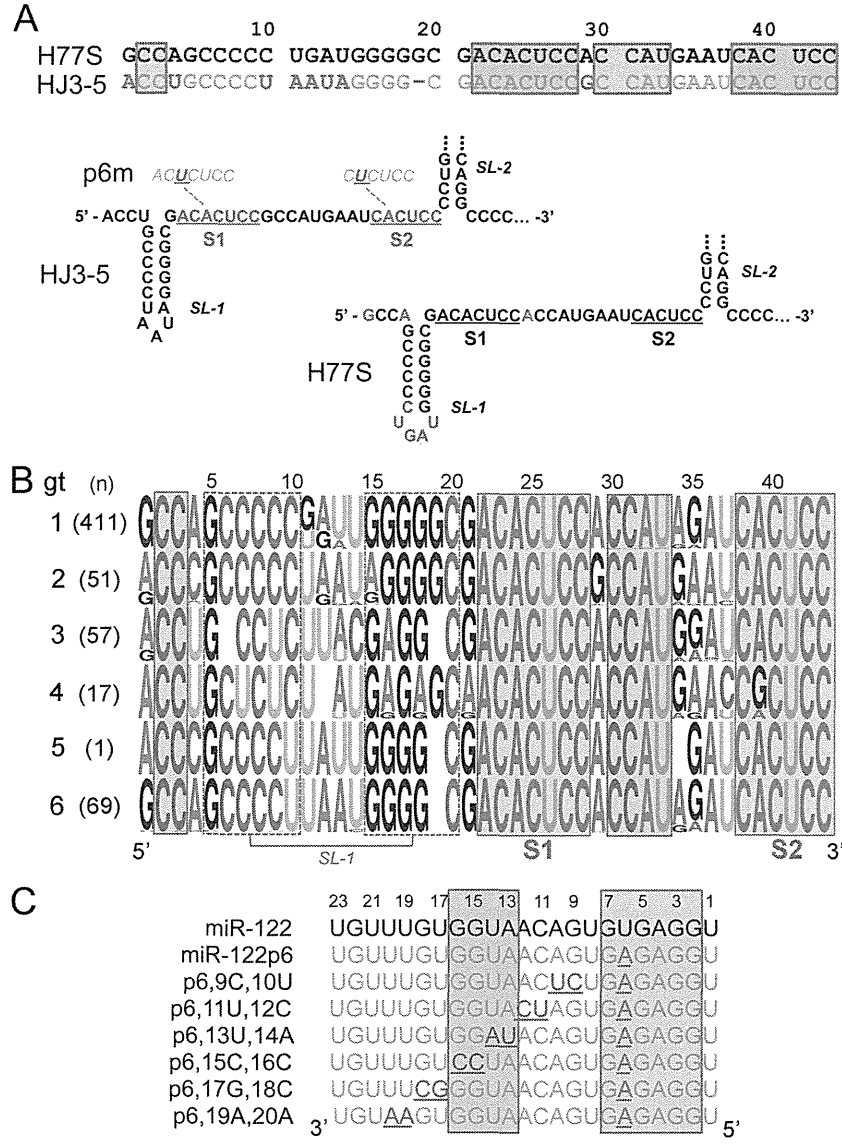


**FIG 1** Conserved complementary sequences near the 5′ end of the HCV genome suggest supplementary binding of miR-122 to HCV RNA 3′ of the miR-122 seed sequences at both S1 and S2. (A) (Top) Alignment of the terminal 5′UTR sequences in H77S (genotype 1a) and HJ3-5 (genotype 2a; derived from JFH-1) viruses. Conserved sequences known to base pair with the seed sequence of miR-122 are highlighted in red boxes. Additional conserved sequences complementary to miR-122 are highlighted in green. Nucleotides in HJ3-5 that differ from those in H77S are shown in red font. (Bottom) Putative secondary structure of the RNA segments, showing stem-loop 1 (SL-1) and the base of stem-loop 2 (SL-2). The S1 and S2 seed match sequences are highlighted in red in the HJ3-5 sequence, with the single base changes in the p6m mutants of S1 and S2 shown above. Bases that differ between the genotype 1a and 2a sequences are highlighted in red in the H77S structure. (B) Logo depiction of sequence conservation in the 5′UTRs of different HCV genotypes. The number and height of each character reflect the diversity in bases and conservation of sequence at each position. Highly conserved sequences are highlighted in red and green as in panel A. Base-paired segments in stem-loop SL-1 are shown in open boxes. The number of sequences of each genotype studied is shown to the left. (C) Guide-strand sequences of miR-122 mutants and related mutants. Point mutations are shown in red. Passenger-strand sequences (Table 1) were modified to maintain the melting temperature of each duplex between 54.3 and 54.9°C. Bases are numbered in a 5′-to-3′ fashion at the top but shown in a 3′-to-5′ manner to facilitate visualization of base pairing with positive-strand HCV RNA. Nucleotides involved in base pair interactions are shaded in red and green as in panels A and B.

fully explain the requirement for miR-122 (15). These data suggest that miR-122 promotes HCV replication by a mechanism other than translation, stabilizing the viral RNA or possibly promoting the initiation of new viral RNA synthesis (15, 28). Consistent with this prediction, we recently confirmed that binding of miR-122 results in the recruitment of an Ago2-containing RISC-like complex that physically stabilizes the viral RNA genome (26). This miR-122–Ago2 complex slows the decay of positive-strand HCV RNA both in RNA-transfected cells and in cells persistently infected with HCV, most likely by protecting the RNA from 5′-exonuclease attack (26).

In addition to base pairing involving the seed sequence, the recognition of cellular mRNA targets by miRNAs may also entail supplementary or accessory interactions of bases 3′ of the seed sequence (1, 12). Such additional base pairing optimally involves nt 13 to 16 and spares nt 9 to 12 of the miRNA, presumably be-

cause such base pairing does not require helix formation throughout the length of the guide strand (as occurs with perfectly complementary small interfering RNA [siRNA]) and thus may not perturb its association with Ago in the RISC (1, 12). Several recent reports provide evidence that the interaction of miR-122 with HCV RNA similarly involves such 3′ supplementary interactions (20, 22, 24). Although details differ between these studies, these interactions appear to contribute to the ability of miR-122 to promote the amplification of HCV RNA in transfected cells or protein expression from reporter RNAs containing the HCV IRES in their 5′UTR. Here we confirm and extend these observations, using a genetic approach to demonstrate 3′ supplementary base pair interactions between miR-122 and the 5′ termini of both genotype 1a and genotype 2a viral RNAs. We show that 3′ supplementary base pairing contributes to the recruitment of Ago2 and the stabilization of HCV RNA by miR-122 and that it is also required for optimal production of infectious virus in cell culture.

## MATERIALS AND METHODS

**Cells.** Huh-7, Huh-7.5, and FT3-7 cells (a clonal derivative of Huh-7 cells) were maintained as described previously (15, 25). Murine embryo fibroblasts (MEFs) were the kind gift of Alexander Tarakhovsky, Rockefeller University, and were maintained in cell culture as described previously (21).

**Plasmids.** pHJ3-5 (19), the related S1, S2, and S1-S2 p6m mutants (15), and pH77S/GLuc2A-AAG (25, 30) have been described previously. The *Gaussia princeps* luciferase (GLuc) coding sequence, followed by the foot-and-mouth disease virus 2A sequence, was inserted between p7 and NS2 in pHJ3-5 or pH77S.3 and the related S1, S2, and S1-S2 p6m, S1p3m, and S1p23m miR-122 binding site mutants, using the strategy adopted previously for H77S (25). Single- and multiple-base substitutions were created within pHJ3-5 and pHJ3-5/GLuc2A by site-directed mutagenesis of the segment spanning the EcoRI and AgeI sites. Base substitutions were similarly introduced into pH77S.3/GLuc2A and pH77S/GLuc2A-AAG by site-directed mutagenesis of the sequence spanning the NotI and AgeI sites. Base changes and the integrity of the surrounding sequences were confirmed by DNA sequencing.

**RNA transcription.** RNA transcripts were synthesized *in vitro* as described previously (25).

**RNA oligonucleotides.** RNA oligonucleotides have been described previously (15) and were synthesized by Dharmacon. Additional mutant miRNAs used in this study are shown in Table 1. All miRNAs were transfected as duplexes (15).

**miRNA supplementation and HCV replication.** FT3-7 cells seeded previously into a 6-well culture plate were transfected with a miRNA duplex (50 nM) by use of Lipofectamine 2000 (Invitrogen) as recommended by the manufacturer. At 24 h, the cells were retransfected with replication-competent *in vitro*-transcribed HCV RNA (1.25 μg/well) for 6 h, using the TransIT mRNA transfection reagent (Mirus Bio) according to the manufacturer's suggested protocol. The cells were retransfected with miRNA 24 h later and refed fresh medium every 24 h thereafter. Supernatant fluid samples were collected for virus titration or GLuc assay at 24-h intervals, unless noted otherwise. Total cellular RNA was extracted for Northern blots.

**miRNA supplementation and HCV RNA stability and translation.** Synthetic HCV RNA containing a replication-lethal mutation in the NS5B coding region (20 μg) and duplex miRNA (1 μM) were mixed with $1 \times 10^7$ wild-type (wt) MEF cells in a 4-mm cuvette and pulsed once at 400 V, 250 μF, and infinite Ω in a Gene Pulser Xcell Total system (Bio-Rad). Synthetic capped and polyadenylated RNA encoding *Cypridina* luciferase (CLuc) was cotransfected to monitor transfection efficiency. The cells were plated into three wells of a six-well culture plate, and cell culture supernatant fluid was collected for GLuc assay and total cellular RNA extracted for Northern blotting at 3-h intervals.

TABLE 1 miR-122 mutants used in this study

| miR-122 mutant | Guide (5′-3′) and passenger-strand (3′-5′) RNA sequences[a] |
|---|---|
| miR-122 | UGGAGUGUGACAAUGGUGUUUGU<br>AUAAAUCACACUAUUACCGCAAA |
| miR-122p6 | UGGAGAGUGACAAUGGUGUUUGU<br>AUAAAUCACACUAUUACCGCAAA |
| miR-122p6,9C,10U | UGGAGAGUCUCAAUGGUGUUUGU<br>AUAAAUCACAGAAUUACCGCAAA |
| miR-122p6,11U,12C | UGGAGAGUGAUCAUGGUGUUUGU<br>AUAAAUCACACUAUUACCGCAAA |
| miR-122p6,13U,14A | UGGAGAGUGACAUAGGUGUUUGU<br>AUAAAUCACACUAUAUCCGCAAA |
| miR-122p6,15C,16C | UGGAGAGUGACAAUCCUGUUUGU<br>AUAAAUCACACUAUUAGGGCAAA |
| miR-122p6,17G,18C | UGGAGAGUGACAAUGGGCUUUGU<br>AUAAAUCACACUAUUACCUGAAA |
| miR-122p6,19A,20A | UGGAGAGUGACAAUGGUGAAUGU<br>AUAAAUCACACUAUUACCGCUUA |
| miR-122m15C,16C | UGGAGAGUGACAAUCCUGUUUGU<br>AUAAAUCACACUAUUAGGGCAAA |

[a] The top sequence for each mutant represents the guide strand, and the lower sequence represents the passenger strand. Underlined bases have been mutated from the wild-type sequence.

**Infectious virus titration.** Huh-7.5 cells were transfected with duplex miR122p6 (50 nM) and then seeded into 48-well plates at a density of $5 \times 10^4$ cells/well and maintained in a 37°C 5% $CO_2$ environment. At 24 h, the cells were inoculated with serial dilutions of virus-containing medium (100 μl). Cells were fed 300 μl fresh medium 24 h later. Following 48 h of additional incubation, cells were fixed, labeled with HCV core-specific antibody, and examined under an inverted UV fluorescence microscope as described previously (25, 30). Clusters of infected cells identified by specific staining for core antigen were considered to constitute a single infectious focus-forming unit (FFU); virus titers are reported as FFU/ml.

**Ago2-RNA immunoprecipitation (IP).** MEFs were electroporated with 10 μg HCV RNA and 1 μM duplex miRNAs. Six hours later, cells were harvested in lysis buffer (150 mM KCl, 25 mM Tris-HCl, pH 7.4, 5 mM EDTA, 1% Triton X-100, 5 mM dithiothreitol [DTT], Complete protease inhibitor cocktail [Roche], 100 U/ml RNaseOUT [Invitrogen]). Lysates were centrifuged for 30 min at 17,000 × *g* at 4°C, filtered through a 0.45-μm syringe filter, and incubated with anti-Ago2 monoclonal antibody (MAb) (2D4; Wako Chemicals) or isotype control IgG at 4°C for 2 h, followed by the addition of 30 μl of protein G Sepharose (GE Healthcare) for 1 h. The Sepharose beads were washed 3 times in lysis buffer, and RNA was extracted using an RNeasy minikit (Qiagen). HCV RNA associated with Ago2 protein was detected by reverse transcription-PCR (RT-PCR), using a SuperScript One-Step RT-PCR kit with Platinum *Taq* DNA polymerase (Invitrogen) and primers specific for the HCV core sequence as described previously (25).

**Luciferase assay.** Cell culture supernatant fluids were collected at 24-h intervals following RNA transfection and replaced completely with fresh medium. Secreted GLuc and CLuc activities were measured as described previously (25).

**Northern blotting.** Northern blotting for HCV RNA and actin mRNA (loading control) and quantitation of these results were carried out as described previously (15, 25).

**Genotype-specific HCV 5′UTR sequence logos.** HCV 5′UTR sequences of at least 300 bases were retrieved from the European HCV database (euHCVdb [http://euhcvdb.ibcp.fr/euHCVdb/]) (4). Genotype-specific (27) sequence alignments were computed using ClustalW (3) and MUSCLE (7), with minor manual modifications in the SeaView alignment editor (11). Sequence logos were computed using WebLogo (http://weblogo.berkeley.edu/logo.cgi) (5).

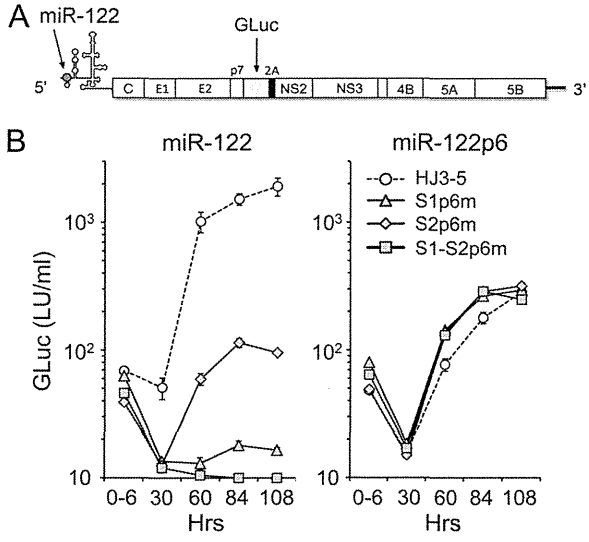


FIG 2 Replication of HJ3-5 RNAs with or without point mutations in the S1 and S2 seed match sites. (A) Organization of synthetic GLuc-expressing HCV genomic RNAs. The GLuc sequence was inserted downstream of p7, followed by the 2A sequence of foot-and-mouth disease virus. (B) GLuc activities in supernatant fluids of cultures transfected with HJ3-5 or related S1 and S2 mutant RNAs and either wt miR-122 (left) or the miR122p6 mutant (right). FT3-7 cells were transfected with the oligoribonucleotides 24 h before and after transfection of the viral RNAs. Supernatant fluids were collected to assay GLuc secreted into the medium between 0 and 6 h following HCV RNA transfection and over successive 24-h periods ending at 30, 60, 84, and 108 h posttransfection. Results shown represent the mean ratios of GLuc activities in replicate cultures ± ranges and are representative of multiple independent experiments. LU, light units.

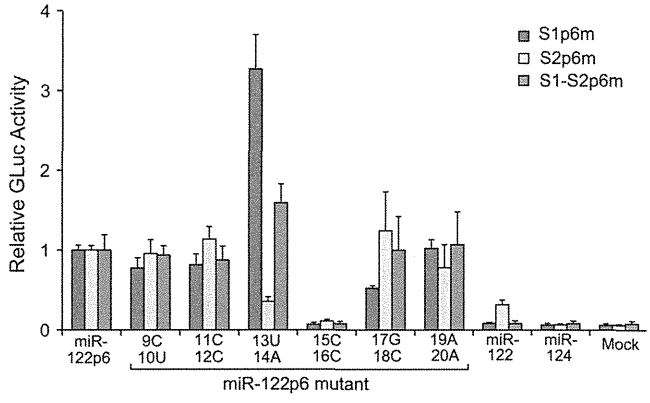


FIG 3 Capacity of various miR-122 mutants to support HCV RNA replication. HJ3-5 RNAs bearing either single or double S1 and S2 p6m mutations, as indicated, were cotransfected into cells with the indicated wt or mutant duplex miR-122s, using the same protocol as that described in the legend to Fig. 2B. Results shown represent the mean ratios of GLuc activities in triplicate cultures at 84 h ± standard deviations (SD), normalized for each viral RNA to that obtained with miR-122p6. The data shown are representative of multiple independent experiments. Mock, no oligonucleotide.

## RESULTS

**miR-122 bases involved in productive interactions with HCV RNA.** A conserved CCAU sequence (HCV nt 30 to 33) upstream of the S2 site in HCV RNA (Fig. 1A, top panel) is complementary to nt 13 to 16 of miR-122 and is thus available for base pairing with the miRNA 3′ of its seed sequence (miR-122 nt 2 to 7) (12). In addition, a conserved CC sequence (HCV nt 2 and 3) upstream of stem-loop 1 represents a similar potential site of 3′ supplementary base pairing at S1. An analysis of over 600 individual viral sequences deposited in the European HCV database (euHCVdb) indicated that these miR-122-complementary bases are highly conserved across all 6 HCV genotypes (Fig. 1B). As indicated above, Machlin et al. (20) recently showed that 3′ supplementary interactions involving nt 15 and 16 of miR-122 and nt 2 and 3 and nt 30 and 31 of the viral RNA contribute to the ability of miR-122 to promote the accumulation of viral RNA following its transfection into permissive cells (20). To further characterize supplementary base pairing of miR-122 outside its seed sequence to HCV RNA, we synthesized a panel of miR-122 mutants in which successive pairs of bases, starting at nt 9 and 10 and going through nt 19 and 20, were replaced with their Watson-Crick complement (Fig. 1C) (the analysis of miR-122 mutants with base substitutions at nt 21 to 23 will be reported elsewhere). Each of these mutated miR-122s had a U-to-A substitution at nt 6 ("p6" mutation). We tested the ability of the mutants, transfected as duplex miRNAs into HCV-permissive FT3-7 cells, to promote the replication of HCV RNA carrying complementary substitutions ("p6m") (Fig. 1A, bottom panel) within the S1, S2, or both S1 and S2 seed sequence binding sites (15). HCV RNAs with a p6m base substitution in either S1 or S2 are severely handicapped in replication, especially when the mutation is at the S1 site, but can be rescued by transfection of the complementary miR-122 p6 mutant (15). This strategy functionally isolates the S1 and S2 miR-122 binding sites, allowing requirements for miR-122 sequence to be determined individually at each seed match site, and is similar to the strategy we used previously to dissect the contributions of the two sites to miR-122-mediated increases in viral translation versus replication (15). Where necessary, the passenger-strand RNA in the duplex was modified to maintain a melting temperature for each duplex that was similar to that of the parental miR-122p6 duplex (Table 1).

The genome-length HCV RNA used in this series of experiments was HJ3-5 (19), a chimera that contains the genotype 2a 5′UTR sequence rather than the genotype 1a H77 5′UTR sequence studied by Machlin et al. (20) (see Fig. 1A for a comparison of the relevant sequences). It was modified by the insertion of the GLuc (*Gaussia princeps* luciferase) sequence within the polyprotein, which allows replication to be monitored by measuring GLuc activity secreted into supernatant fluids of transfected cell cultures (Fig. 2A). As expected (15), viral RNAs with p6m mutations in S1 or S2 produced much less GLuc than RNAs containing the wt seed match sequences when cotransfected into cells with wt miR-122 (Fig. 2B, left panel). The GLuc expression pattern suggested a lack of replication of the double S1-S2p6m mutant. In contrast, the GLuc activity produced by each of these RNAs was substantially increased when the RNAs were cotransfected with miR-122p6 (Fig. 2B, right panel), with the S1-S2p6m mutant replicating with an efficiency similar to that of the other RNAs.

Each of the modified miR-122p6 duplexes (Fig. 1C) was cotransfected into cells with either the S1p6m, S2p6m, or S1-S2p6m HJ3-5 HCV RNA, and GLuc activity secreted into the culture supernatant fluids was monitored over the ensuing 84 h as a measure of genome amplification. The results are presented in Fig. 3, which shows the GLuc activity at 84 h posttransfection, normalized for each of the viral RNAs to that produced by cotransfection with miR-122p6 (which lacks base substitutions outside the seed

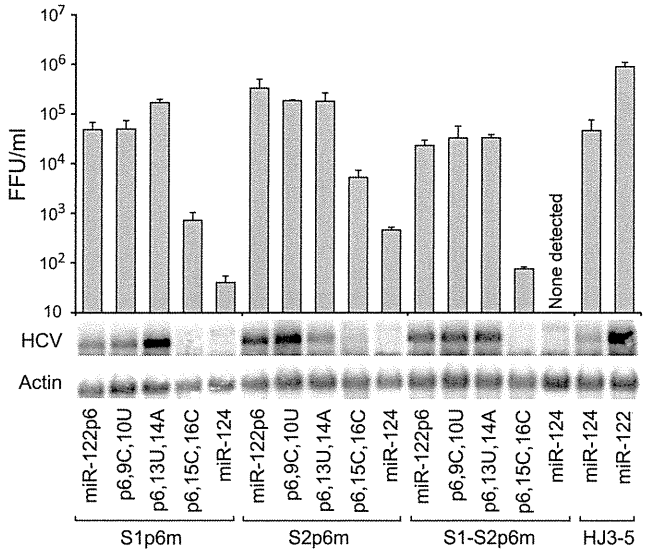


**FIG 4** miR-122 nt 13 to 16 are essential for support of HCV RNA replication and production of infectious virus in cell culture. (Top) FT3-7 cells were transfected with HJ3-5 RNA and related p6m mutants 24 h after transfection with the indicated duplex oligoribonucleotides and then retransfected 24 h later with the same oligoribonucleotides. After an additional 48 h of incubation, supernatant fluids were harvested for titration of HCV infectivity in a focus-forming assay using Huh-7.5 cells transfected with miR-122p6 24 h prior to inoculation. (Bottom) RNA extracted from the HCV RNA-transfected cells was subjected to Northern analysis for HCV RNA. β-Actin mRNA served as a loading control.

sequence). As additional controls, the HCV RNA-transfected cells were also supplemented with wt miR-122 or miR-124, an unrelated brain-specific miRNA. miR-122p6 mutants with base substitutions in nt 9 to 12 and 17 to 20 functioned as well as miR-122p6 in promoting genome amplification, indicating that these bases are not important for the interaction with HCV RNA. However, very different results (either decreased or increased GLuc expression) were obtained with miR-122p6 mutants with base substitutions at nt 15 and 16 or nt 13 and 14 (Fig. 3). miR-122p6,15C,16C was markedly impaired in the ability to rescue the amplification of HCV RNAs with p6m mutations at either the S1 or S2 site (Fig. 3). In contrast, while miR-122p6,13U,14A had a significantly reduced capacity to rescue amplification of the S2p6m mutant, it demonstrated 3-fold greater activity than miR-122p6 in promoting replication of the S1p6m RNA and was able to enhance replication of the double S1-S2p6m mutant (Fig. 3). Northern blotting of RNAs extracted from cells transfected with HJ3-5 virus RNAs containing only the miR-122 binding site mutations (no GLuc2A insertion) confirmed these results, as well as the absence of any effect of substitutions at miR-122 nt 9 and 10 (Fig. 4, bottom panels).

The marked decrease we observed in the ability of the miR-122p6,15C,16C mutant to promote amplification of HCV RNA with a genotype 2a 5′UTR confirms the loss of activity of a similar miR-122 mutant against genotype 1a RNA reported by Machlin et al. (20) and is consistent with 3′ supplementary base pair interactions between miR-122 and bases upstream of both the S1 (nt 2 and 3) and S2 (nt 30 and 31) sites in the viral RNA (as suggested in Fig. 1). However, the results we obtained with miR-122 mutated at nt 13 and 14 were quite different from those described previously for a genotype 1 virus. Machlin et al. (20) reported an ~70% decrease in the ability of a similar miR-122 mutant to promote HCV RNA accumulation when bound at the S1 seed match site, while we observed a >3-fold increase in activity (Fig. 3). We show below that these differences, which are large and very significant for miRNA activities, reflect genotype-specific variation in the 5′UTR sequences used in the two studies.

**Base substitutions in miR-122 and promotion of infectious virus yield.** Since prior studies have not determined the relevance of 3′ supplementary miR-122 mutations to the production of infectious virus, we measured the yields of infectious virus produced from cells cotransfected with the HJ3-5 S1p6m, S2p6m, or S1-S2p6m RNA and key miR-122p6 mutants. Although the dynamic range of the FFU assay used for titration of infectious virus is far greater (extending over >4 orders of magnitude) than that of Northern blotting for HCV RNA, the results generally mirrored each other (Fig. 4). There was no detectable virus produced by the double S1-S2 mutant RNA in the absence of cotransfected miR-122p6. Virus yields from the single S1 and S2 mutants were also very low, but production of infectious virus from each of these HCV RNAs was boosted 100- to 1,000-fold by cotransfection with miR-122p6. In contrast, miR-122p6,15C,16C was severely impaired in the ability to support production of infectious virus by each of the three HJ3-5 mutants. Nonetheless, it did cause an approximately 10-fold increase in infectious virus yield compared with miR-124, indicating that 3′ supplementary base substitutions involving nt 15 and 16 of miR-122 are not absolutely essential for the interaction with HCV RNA and for miR-122 boosting of infectious virus production. The base substitutions at nt 13 and 14 had less impact on infectious virus yield. However, cotransfection of miR122p6,13U,14A with the S1 mutant RNA resulted in a significant increase in virus yield compared with that with miR122p6 and in a slight reduction of yield compared to that with the S2 mutant. These results are consistent with the GLuc results obtained in the transient-transfection experiments shown in Fig. 3. Although disruption of miR-122 binding at either the S1 or S2 binding site has a strong negative effect on viral RNA amplification and infectious virus yields, the results shown in Fig. 4 confirm a greater dependency on the S1 versus S2 seed match site for virus replication, as we suggested previously (15).

**Complementary mutations at HCV nt 2 and 3 and nt 30 to 33 rescue miR-122 mutants with substitutions at nt 13 to 16.** The strong negative impact of cytosine-for-guanine substitutions at nt 15 and 16 of miR-122 in the experiments described above is consistent with miR-122 base pairing to the conserved cytosines at positions 2 and 3 and positions 30 and 31 in HCV RNA (Fig. 1). This was confirmed by Machlin et al. (20), who demonstrated rescue of miR-122 promotion of viral RNA accumulation when mutations complementing base substitutions at nt 15 and 16 of miR-122 were constructed within the viral RNA. However, the negative impact of the 13U and 14A substitutions observed with miR-122 interactions at the S2 site (Fig. 3) suggested that the supplementary base pairing upstream of S2 extends in a 3′ direction on the viral RNA, to include nt 32 and 33. To confirm this, we constructed HJ3-5/GLuc2A-S2p6m RNAs with base substitutions at nt 32 and 33 that were complementary to those in miR-122p6,13U,14A. We also constructed viral RNAs with guanine substitutions at nt 2 and 3 and nt 31 and 32 to complement the base changes in the miR-122p6,15C,16C mutant. The replication of each of these viral RNA mutants was impaired compared with

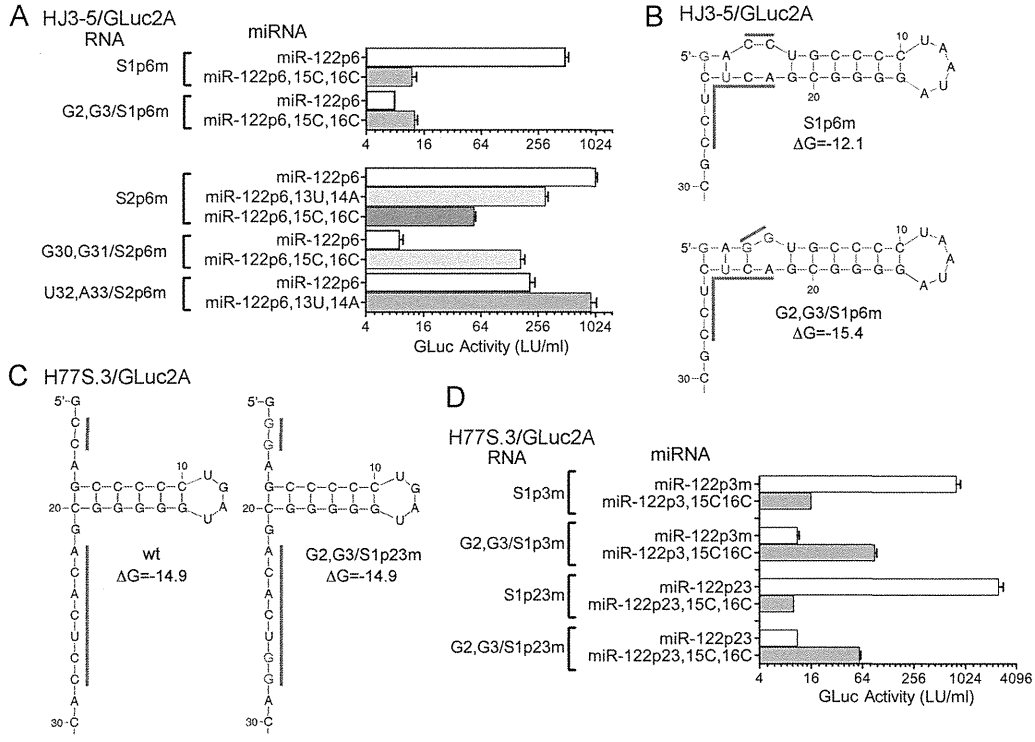


**FIG 5** Functional rescue of miR-122 mutants by complementary substitutions in HCV RNA. (A) Complementary substitutions at nt 2 and 3 and nt 30 to 33 of HCV RNA rescue promotion of its amplification by miR-122p6 mutants with substitutions at nt 13 and 14 and/or nt 15 and 16. Replication-competent HJ3-5/GLuc2A RNAs with p6m mutations in S1 (top) or S2 (bottom) and additional base substitutions at nt 2 and 3, 30 and 31, or 32 and 33 were transfected into FT3-7 cells with the indicated oligoribonucleotides, as described in the legend to Fig. 2. Results shown represent mean GLuc activities in supernatant fluids 96 h following transfection ± ranges. Minimal but statistically significant rescue was observed with S1p6m RNA, while rescue was relatively efficient with S2p6m RNA. (B) mfold prediction of secondary structure at the 5′ end of the HJ3-5/GLuc2A-S1p6m transcripts with and without complementary G2 and G3 substitutions. Note that the first guanine base is generated from the T7 promoter sequence in the plasmid, whereas the first nucleotide of H77S is naturally guanine (see Fig. 1). (C) mfold predictions of secondary RNA structures of H77S.3/GLuc2A and H77S.3/GLuc2A-G2,G3-S1p23m. (D) Ability of complementary mutations in H77S.3/GLuc2A-S1p3m and -S1-p23m RNAs to rescue activity of cognate miR-122 mutants with 15C and 16C substitutions.

that of the cognate HJ3-5/GLuc2A-S1p6m or -S2p6m parent (as determined by GLuc expression in transient-transfection assays) (Fig. 5A), with the G2,G3 and G30,G31 mutants affected more than the U32,A33 mutant. With each mutant, the reduction in replication capacity was rescued at least partially by cotransfection with miR-122p6,15C,16C (G2,G3 and G30,G31 mutants) or miR-122p6,13U,14A (U32,A33 mutant). These results provide genetic evidence for the suspected supplementary base pairing, including its extension to nt 32 and 33 as suggested in Fig. 1B.

While we observed a reproducible, ~2-fold enhancement in GLuc expression from HJ3-5/GLuc2A-S1p6m,G2,G3 when it was cotransfected with its cognate miR-122p6,15C,16C mutant, its replication remained very inefficient. One possible explanation for this is an aberrant RNA secondary structure when guanines are inserted in lieu of the cytosines at positions 2 and 3 in the genotype 2a 5′UTR. mfold predictions (http://mfold.rna.albany.edu) of secondary structure in the HJ3-5/GLuc2a-S1p6m,G2,G3 mutant RNA suggest that it forms a stable stem-loop ($\Delta G = -15.4$ kcal) at its extreme 5′ end (Fig. 5B). We considered this a likely explanation for the lack of complete rescue of replication with the complementary miR-122 mutant, since Machlin et al. (20) did not report any difficulty in rescuing a similar mutant genotype 1a RNA. To confirm this, we constructed two G2,G3 mutants constructed in the background of H77S.3/GLuc2A, in which the viral sequence is entirely genotype 1a. In addition to the G2,G3 substitutions, we made base changes at position 3 or both positions 2 and 3 in the S1 seed match site (p3m and p23m mutants). None of these mutations alter the predicted secondary structure at the 5′ end of the genotype 1a genome (Fig. 5C). Despite this, cotransfection of the complementary miR-122p3,15C,16C and miR-122p23,15C,16C mutants with these HCV mutants only partially rescued the large defect in replication capacity imposed by the G2,G3 substitutions (Fig. 5D). We concluded that while these bases are engaged in supplementary 3′ base pairing with miR-122, there is an additional requirement for cytosines at positions 2 and 3. One possibility is that these bases are involved in recognition of the 5′ end of the genome by the HCV replicase (9).

**3′ supplementary base pair interactions are required for miR-122 stabilization of HCV RNA.** We have shown recently that binding of a miR-122–Ago2 complex stabilizes HCV RNA and results in decreased rates of decay of both synthetic viral RNA transfected into cells and replicating viral RNA in infected cells (26). To determine whether 3′ supplementary base pair interactions of miR-122 contribute to this stabilizing action, we monitored RNA decay in cells cotransfected with a replication-incompetent HCV RNA and various miR-122 mutants. We used MEFs for these experiments because they do not express miR-122. This ensures that results are not confounded by expression of endogenous miR-122. Cells were transfected with genotype 1a H77S RNA modified to express GLuc and containing a replication-lethal mu-

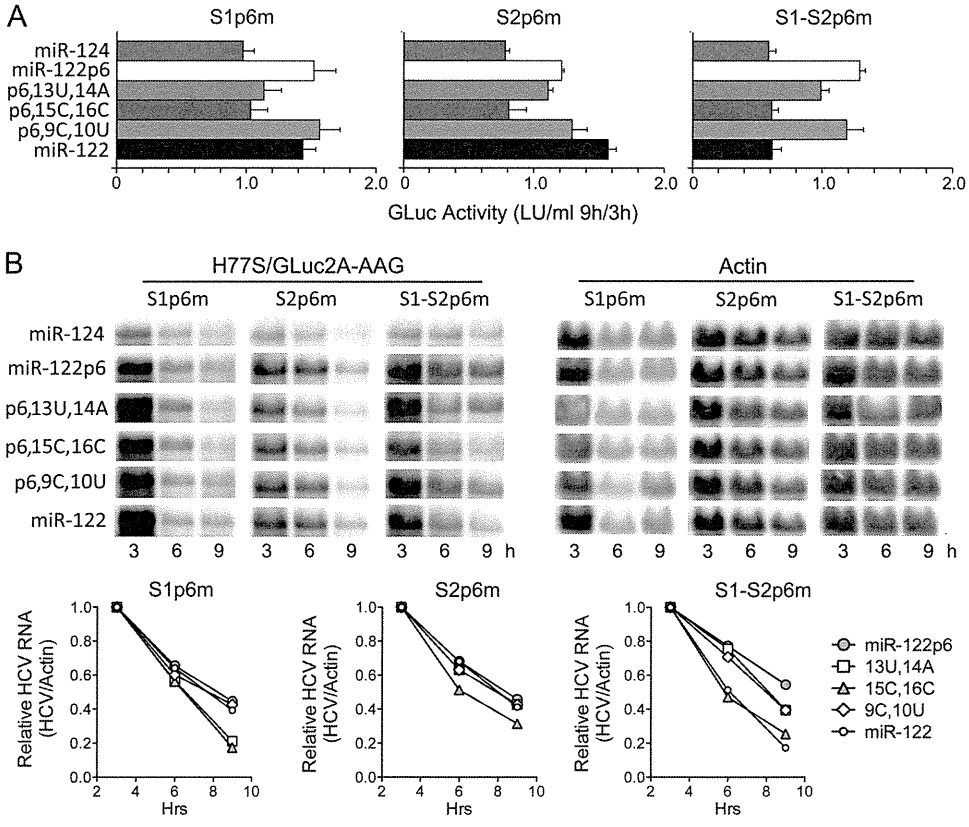


**FIG 6** 3′ supplementary interactions involving nt 13 to 16 contribute to stabilization of HCV RNA by miR-122. (A) GLuc expression from replication-incompetent, genotype 1a H77S/GLuc2A-AAG and related p6m S1 and S2 mutant RNAs that were coelectroporated into MEFs with the indicated miR-122 duplexes. Results shown represent the means ± ranges of the ratios of GLuc activities in supernatant fluids from duplicate transfected cultures at 9 h versus 3 h and are representative of replicate experiments. (B) Northern analysis of HCV RNA and β-actin mRNA (loading control) in RNAs extracted from cells 3, 6, and 9 h after electroporation of the indicated viral RNAs and duplex miRNAs. Quantitation of HCV RNA (HCV/actin mRNA) in representative Northern blots is shown below, normalized to that present at 3 h (arbitrarily set to 1.0), to compare the stability of the RNA cotransfected with different miR-122 mutants.

tation within the NS5B coding sequence (H77S/GLuc2A-AAG). As we have shown previously (25), GLuc expression from this RNA results exclusively from translation of the input RNA, peaking at around 3 h posttransfection. Thus, the ratio of GLuc activity in culture supernatant fluids at 9 h versus 3 h posttransfection reflects the rate of decay of the transfected RNA (25). p6m mutations were placed within the S1 or S2 seed match sites, as described above (Fig. 1A). As expected, the ratio of GLuc activity expressed by cells transfected with the H77S/GLuc2A-AAG/S1-S2p6m double mutant at 9 h versus 3 h was enhanced when the mutant was cotransfected with miR-122p6 but not miR-122 or the control, brain-specific miR-124 (Fig. 6A, right panel). miR-122p6,9C,10U was as capable as miR-122p6 at enhancing the level of GLuc expression at 9 h versus 3 h, but miR-122p6,15C,16C was no more active than miR-124 or miR-122. These results are consistent with our earlier observations that base pairing involving nt 15 and 16 of miR-122 is required for efficient replication of HJ3-5 RNA (Fig. 3 to 5). Stabilization of the HCV RNA was confirmed by Northern blots of total cellular RNA extracted 3, 6, and 9 h after transfection. These results showed greater abundance of the viral RNA at 9 h when it was cotransfected with miR-122p6 or miR-122p6,9C,10U than when it was cotransfected with miR-122p6,15C,16C, miR-122, or miR-124 (Fig. 6B).

In contrast to miR-122p6,15C,16C, miR-122p6,13U,14A demonstrated only a modest reduction in the ability to promote GLuc expression at 9 h versus 3 h (compared to that of miR-122p6) (Fig. 6A, right) or in the ability to stabilize the S1-S2p6m RNA in Northern blots (Fig. 6B). Thus, while base pairing at nt 13 and 14 of miR-122 contributes to the stabilization of viral RNA, it appears to be less important than the interactions involving nt 15 and 16.

We also examined the ability of the mutated miRNAs to stabilize H77S/GLuc2A-AAG RNA with mutations within either the S1 or S2 seed match sites. Unlike the case for the double S1-S2p6m mutant, GLuc assays (Fig. 6A, left and center panels) and Northern blots (Fig. 6B) revealed that these mutants were both stabilized by wild-type miR-122. This likely reflects interactions with the alternative, nonmutated binding site (e.g., the S2 site in the S1p6m mutant) and is consistent with both miR-122 binding sites contributing to stabilization of the RNA. As expected, the miR-122p6,15C,16C mutant had a smaller effect than that of the control (miR-122p6) on the stability of either the S1p6m or S2p6m mutant, based on GLuc expression (Fig. 6A) and HCV RNA abundance at 9 h (Fig. 6B). Base pairing of nt 15 and 16 at both binding sites is thus important for stabilization. However, in contrast to the substantial enhancement we observed with miR-122p6,13U,14A relative to miR-122p6 in promoting replication of the HJ3-5/GLuc2A-S1p6m mutant (Fig. 2 and 3), miR-122p6,13U,14A was less active

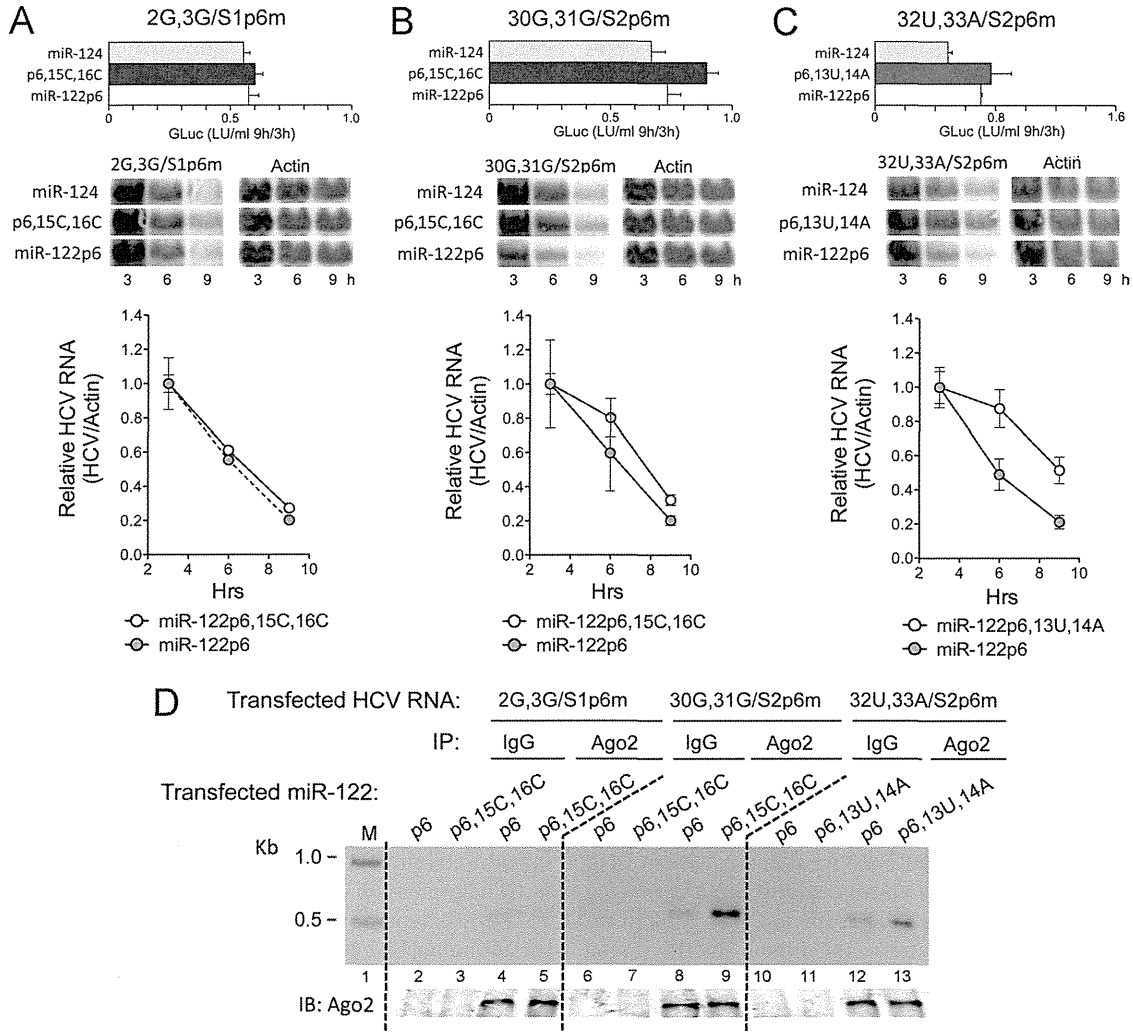


**FIG 7** Complementary mutations at HCV nt 30 and 31 restore a stabilization phenotype to miR-122p6 mutants with base substitutions at positions 15 and 16. H77S/GLuc2A-AAG RNAs carrying an S1 or S2 p6m mutation and additional nucleotide substitutions at nt 2 and 3 (A), nt 30 and 31 (B), or nt 32 and 33 (C) were transfected into MEFs with the indicated miRNA duplexes. The top panel of each of these figures shows the ratio of GLuc activity at 9 h versus 3 h. The middle panels show Northern blots of the HCV RNA at 3, 6, and 9 h, with actin mRNA included as a loading control. At the bottom of each panel is shown the quantitation of Northern blotting results from duplicate transfections, comparing HCV RNA to actin mRNA at 3, 6, and 9 h (means ± ranges). Results were normalized to the HCV RNA abundance at 3 h (arbitrarily set to 1.0) in order to compare the stability of the viral RNA cotransfected with miR-122p6 versus the complementary mutant. (D) Ago2-RNA immunoprecipitation results obtained with lysates from cells cotransfected with the mutant HCV RNAs in panels A to C and either miR-122p6 or related mutants.

than miR-122p6 in stabilizing the H77S/GLuc2A-S1p6m mutant (Fig. 6A and B). Subsequent experiments (see below) demonstrated that this difference in the activity of the miR-122p6,13U,14A mutant with the H77S versus HJ3-5 RNA was due to differences in the nucleotide sequences of the two viral RNAs at nt 4.

Additional experiments were carried out to demonstrate whether the mutated miRNAs were capable of stabilizing H77S/GLuc2A-AAG RNAs carrying complementary mutations. These studies revealed that supplementation with miR-122p6,15C,16C resulted in no significant increase in the expression of GLuc 9 h versus 3 h following transfection of 2G,3G/S1p6m RNA compared with that with miR-122p6 (Fig. 7A, top panel). This was confirmed in quantitative Northern blots showing that miR-122p6,15C,16C did not enhance the stability of the 2G,3G/S1p6m RNA (Fig. 7A, middle and bottom panels). This is consistent with the minimal rescue of replication of the 2G,3G/S1p6m mutant by miR122p6,15C,16C (Fig. 5, top panel) and suggests that there may be other factors controlling miR-122 interactions at S1. In contrast, miR-122p6,15C,16C was capable of stabilizing the 30G,31G/S2p6m mutant, as evidenced by GLuc assays and in Northern blots (Fig. 7B), while miR-122p6,13U,14A similarly stabilized 32U,33A/S2p6m RNA (Fig. 7C). These last results provide strong support for the supplemental 3′ base pairing between nt 13 to 16 of miR-122 and the HCV sequence upstream of S2 proposed in Fig. 1, and they indicate its importance in stabilization of the viral genome.

**3′ supplementary interactions of miR-122 with HCV RNA contribute to the recruitment of Ago2.** miR-122-mediated stabilization of HCV RNA is dependent upon recruitment of Ago2 to the viral 5′UTR (26). To ascertain the involvement of the 3′ sup-

plementary base pair interactions in this process, we used RT-PCR to determine whether HCV RNA was physically associated with Ago2 immunoprecipitated from lysates of cells cotransfected with mutated viral RNAs and their cognate miR-122 mutants, as in the experiments shown in Fig. 7A to C. The technical details of these Ago2-RNA co-IP experiments are provided in Materials and Methods and have been published previously (26). The results of these experiments confirmed that base pairing of nt 13 and 14 and nt 15 and 16 of miR-122 with nt 32 and 33 and nt 30 and 31 in HCV, upstream of the S2 seed match site, is important for Ago2 recruitment (Fig. 7D). HCV RNA was enriched in Ago2 precipitates from cells transfected with the 32U,33A/S2p6m and 30G,31G/S2p6m HCV RNAs and the complementary p6,13U,14A and p6,15C,16C miR-122 mutants, respectively, versus miR-122p6, which lacks the relevant complementary base changes (Fig. 7D, lane 13 versus lane 12 and lane 9 versus lane 8). In contrast, very little HCV RNA was coimmunoprecipitated with Ago2 from lysates of cells transfected with the 2G,3G/S1p6m viral RNA, and there was no enrichment of the RNA in cells cotransfected with the complementary p6,15C,16C miR-122 mutant (Fig. 7D, compare lanes 4 and 5). These results are consistent with the inability of complementary miR-122 mutants with base changes at positions 15 and 16 to fully rescue replication and/or stabilization of either genotype 1a or 2a HCV RNA mutants with cytosine-to-guanine mutations at nt 2 and 3 (Fig. 5A and D). Again, these results suggest that the interaction of miR-122 with HCV RNA upstream of the S1 seed match site may be more complex than simple supplementary base pairing between nt 15 and 16 of miR-122 and nt 2 and 3 of HCV RNA.

**Nucleotide 4 of genotype 1 HCV RNA base pairs with nt 14 of miR-122.** The results described above demonstrate a surprising difference in the impact of the miR-122p6,13U,14A mutant on replication of HJ3-5 RNA when the miRNA is bound at the S1 seed match site versus its effect on protein expression and stability of the replication-incompetent H77S RNA. While it was significantly more potent than miR-122p6 in promoting the replication of HJ3-5/GLuc2A-S1p6m RNA (Fig. 3), it had little ability to stimulate translation or to stabilize H77S/GLuc2A-S1p6m RNA (Fig. 6A and B). A comparison of the nucleotide sequences of the H77S (genotype 1a) and HJ3-5 (genotype 2a) 5′UTRs (Fig. 1A) suggested a possible explanation for these contrasting effects. Among other differences, base position 4 is adenine in H77S (and most other genotype 1 viruses) but uracil in HJ3-5 (Fig. 1A). (Note, however, that this base is cytosine in most genotype 2 viruses [Fig. 1B].) The presence of A4 in H77S would allow an extension of base pairing at C2 and C3 to include A4, as it could base pair with U14 of miR-122 (Fig. 8A, top panel). Since this pairing is not possible with the miR-122p6,13U,14A mutant, the loss of this pairing could explain the reduced ability of the latter to promote translation or stabilization of the H77S RNA, as shown in Fig. 6A and B. On the other hand, while the genotype 2a HJ3-5 sequence does not allow base pairing with wild-type miR-122 at this position, it does allow it with the miR-122p6,13U,14A mutant (Fig. 8A, bottom panel). Thus, functionally important base pairing between nt 4 of the HCV genome and nt 14 of miR-122 could explain the increase in replication of the HJ3-5/S1p6m RNA cotransfected with miR-122p6,13U,14A, as shown in Fig. 3.

To determine whether loss of base pairing at nt 4 of the H77S RNA is responsible for the inability of miR-122p6,13U,14A to stabilize this RNA, we replaced the adenine at position 4 of the H77S RNA with a uracil. This mutation restores the potential for base pairing with nt 14 in miR-122p6,13U,14A. As anticipated, it conferred upon miR-122p6,13U,14A the ability to enhance GLuc expression and to stabilize the H77S RNA to a greater extent than that with miR-122p6 (Fig. 8B). These results are supportive of base pairing between nt 14 of miR-122 and nt 4 of the genotype 1 HCV RNA.

To further assess how miR-122 base pairs with the first 4 nucleotides of the genotype 2 5′UTR, we examined the impact of G2,G3 and G2,G3,A4 substitutions in HJ3-5/GLuc2A RNA cotransfected with either wt miR-122 or miR-122m15C,16C. There were no mutations in either seed match sequence in these experiments. The G2 and G3 substitutions resulted in a sharp reduction in replication of the RNA, as determined by GLuc expression 72 h after transfection, and in the absence of any stimulation when the RNA was cotransfected with wt miR-122 (Fig. 8C). However, GLuc expression was approximately doubled when the G2,G3 RNA was cotransfected with miR-122m15C,16C yet still remained much less than that observed with wt HJ3-5 (Fig. 8C). This provides additional support for base pair interactions between nt 2 and 3 of HCV and nt 15 and 16 of the miRNA but again shows that complementary mutations in miR-122 only partially rescue guanine substitutions at nt 2 and 3 of the genome (Fig. 5, top panel). The additional introduction of an adenine substitution at nt 4 resulted in a marked boost in replication when the RNA was cotransfected with miR-122m15C,16C but had no apparent impact when the RNA was cotransfected with wt miR-122 (Fig. 8C). There was also no increase in replication after cotransfection of miR-122m15C,16C when only the A4 substitution was introduced into HJ3-5 RNA, although this led to a 4-fold increase in GLuc expression over that in wt HJ3-5 in the absence of miR-122 supplementation (Fig. 8C). This likely reflects formation of the additional base pair at nt 4 with nt 14 of endogenous miR-122 (Fig. 8D). Consistent with this, replication was further increased when the A4 RNA was cotransfected with wt miR-122. Collectively, these data provide strong support for functionally important base pair interactions between nt 4 of HCV and nt 14 of miR-122. However, this interaction is possible only when the base composition of HCV includes an adenine at nt 4 and is permissive for it (i.e., in genotype 1 and genotype 6 viruses, as shown in Fig. 1B).

## DISCUSSION

The data we present here both confirm and extend previous studies suggesting that bases 3′ of the seed sequence in miR-122 form accessory Watson-Crick interactions with HCV RNA at base positions located upstream of both the S1 and S2 seed match sequences. Previous studies by Machlin et al. (20) demonstrated that the introduction of complementary mutations at HCV nt 2 and 3 and nt 30 and 31 rescued the ability of miR-122 with base substitutions at nt 15 and 16 to promote amplification of a subgenomic genotype 1a HCV RNA in transfected cells. We confirmed this in studies of genome-length RNA possessing a genotype 2a 5′UTR (Fig. 5). However, we provide new genetic complementation data suggesting that functionally important base pairing extends to nt 14 of miR-122 and HCV nt 4 (Fig. 8), upstream of the S1 seed match site, and to nt 13 and 14 of miR-122 and HCV nt 32 and 33, upstream of S2 (Fig. 5). We also extend the understanding of the functional significance of these 3′ supplementary base pair interactions of miR-122 by showing that they are important for the

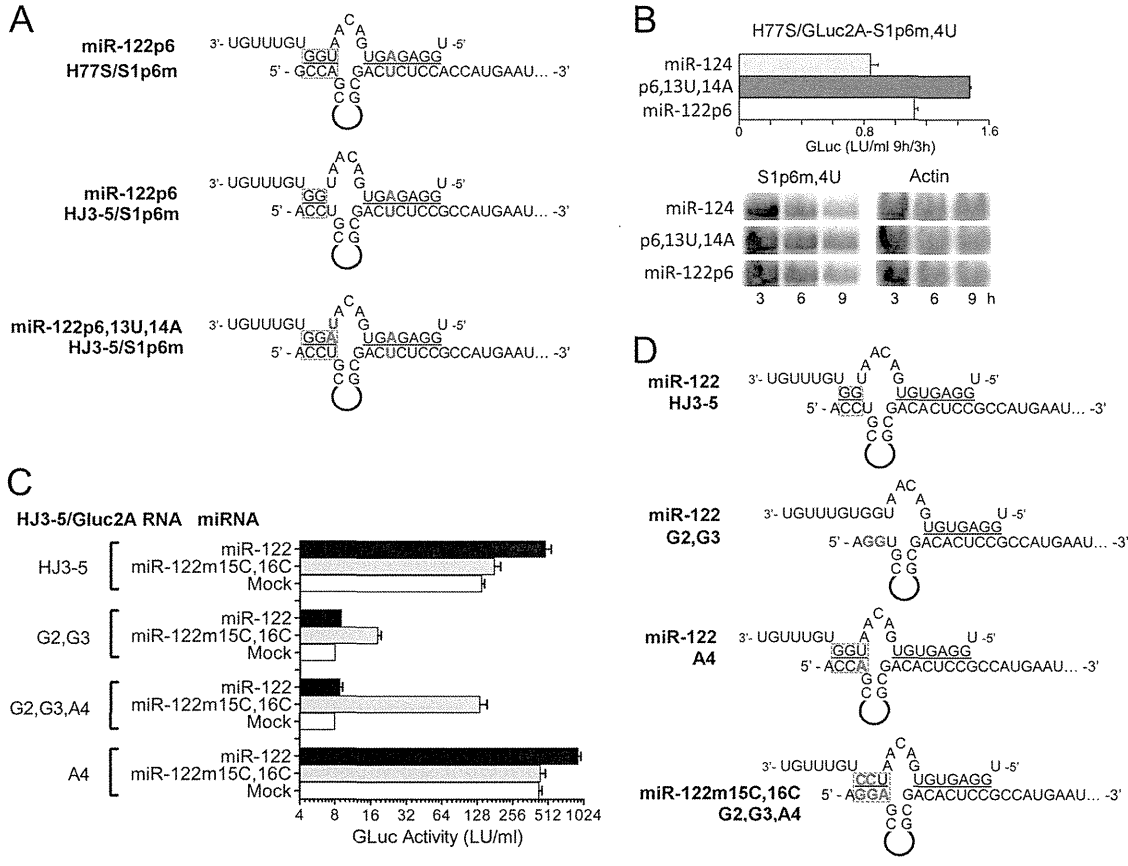


**FIG 8** Influence of HCV nt 4 on the interaction with miR-122. (A) The adenine present at nt 4 of H77S (genotype 1a) (top) RNA provides an opportunity for an additional base pair to form with U14 of miR-122. This is not possible with HJ3-5 (genotype 2a) (middle) RNA, in which nt 4 is uracil. However, U4 of HJ3-5 can pair with A14 of miR-122p6,13U,14A (middle), potentially explaining why this mutant has more activity than wt miR-122 at the S1 site in HJ3-5 (see Fig. 3). (B) Like the case with HJ3-5, miR-122p6,13U,14A has greater activity than wt miR-122 in stabilizing the H77S/GLuc2A-S1p6m,4U mutant. Data shown represent the ratios of GLuc activities at 9 h versus 3 h (top) and Northern blots of the RNA at 3, 6, and 9 h posttransfection. (C) GLuc expressed by FT3-7 cells cotransfected with HJ3-5/GLuc2A or related mutant RNAs with wt miR-122 versus miR-122m15C,16C (no p6m mutation in either). "Mock" indicates no oligoribonucleotide. See the legend to Fig. 6 for additional details. (D) Putative base pair interactions involving nt 2 to 4 of HCV and wt miR-122 or miR-122m15C,16C.

production of infectious virus progeny from RNA-transfected cells (Fig. 4) and that they contribute significantly to the ability of miR-122 to both recruit Ago2 to the viral genome (Fig. 7D) and physically stabilize the viral RNA and lower its rate of decay in cells (26) (Fig. 6 and 7A to C).

For at least a subset of miRNAs, the specificity with which cellular mRNAs are targeted depends partly upon sequences 3′ of the seed sequence (nt 2 to 8). The base pairing that occurs between these miRNAs and their target mRNAs outside the seed sequence typically spares nt 9 to 12 of the miRNA and involves primarily nt 13 to 16 (1, 12). This is likely driven by the architecture of the miRISC and, more specifically, by the need to maintain proper orientation of the miRNA guide strand loaded into an argonaute protein (1). The seed sequence (~nt 2 to 8) is positioned to the exterior of this complex, where it is preoriented in a manner facilitating its base pairing with the mRNA target. The extension of contiguous base pairs beyond nt 8 of the miRNA would result in a helical structure that is likely to disrupt its association with Ago (1). Thus, the lack of involvement of nt 9 to 12 of miR-122 in base pair interactions with the HCV genome, as indicated by our studies, is likely to facilitate continued association of miR-122 with Ago2 yet permit additional base pair interactions, involving nt 13 to 16, that enhance the affinity and specificity of the target interaction. In contrast to our findings, recent studies using selective 2′-hydroxyl acylation analyzed by primer extension (SHAPE) to analyze the impact of miR-122 on the structure of the 5′UTR concluded that base pairing outside the seed sequence at S2 involves nt 9 to 12 of miR-122 (22). This likely reflects the fact that these studies were done *in vitro*, in the absence of Ago2. Supplemental base pairing of miRNAs with their targets 3′ of the seed sequence may not be common (13). However, the pattern of accessory base pair interactions revealed here for miR-122 and HCV RNA at S2 is consistent with what is known of the interaction of miRNAs with their mRNA targets in the context of a loaded miRISC, and thus consistent with miR-122 recruiting Ago2 to the HCV 5′UTR (26).

In addition to genome-length HCV RNAs such as those used in this study, short reporter RNAs containing the authentic 5′- and 3′UTR sequences of HCV have been used to demonstrate a role for miR-122 in promoting translation directed by the HCV IRES, as well as potential 3′ supplementary base pair interactions of miR-122 (14, 24). However, it remains uncertain how well these

reporter RNAs model the interactions of miR-122 with replication-competent viral RNAs. While the potential for base pairing between nt 2 to 4 of a reporter RNA and 3′ miR-122 sequences was demonstrated in a recent study by the loss of miR-122 regulation of reporter activity when substitutions were made at nt 3 and 4 of the reporter, no effect on miR-122 regulation was apparent with substitutions at nt 30 to 34, upstream of the S2 seed match site (24). These results contrast sharply with those shown in Fig. 5A, where the regulation of viral RNA replication by miR-122 was significantly ablated by G30,G31 and U32,A33 substitutions in HJ3-5/GLuc2A RNA yet rescued by complementary mutations in miR-122. These differences demonstrate that studies with short reporter RNAs need to be interpreted with caution and, where possible, confirmed with replication-competent RNAs.

Although our finding that miR-122 nt 15 and 16 are important for replication of genotype 1 HCV RNA (Fig. 3) is in agreement with the work of Machlin et al. (20), we observed substantial differences in the impact of other nucleotide substitutions, particularly at the most 5′ S1 binding site. We found that miR-122p6,13U,14A was >3-fold more potent than miR-122p6 in promoting the replication of HJ3-5/GLuc2A-S1p6m RNA (Fig. 3 and 4), while Machlin et al. (20) reported that a very similar miR-122 mutant had a reduced ability to support HCV RNA replication. This difference is related to variation in the 5′UTR sequences studied. In contrast to its increased ability to promote replication of HJ3-5 RNA, which contains a genotype 2a 5′UTR, the 13U,14A miR-122 mutant was unable to stimulate translation of or stabilize H77S/GLuc2A-S1p6m RNA (Fig. 6A and B), which, like the subgenomic HCV RNA studied by Machlin et al. (20), contains a genotype 1a 5′UTR. This was reversed by replacing the adenine normally present at position 4 of the genotype 1a 5′UTR with the uracil present in genotype 2a viruses (Fig. 8B). These results thus demonstrate that there are genotype-specific differences in base pairing of HCV RNA with miR-122. They also show that there is a potential for productive base pair interactions at nt 4 of genotype 1 and 6 HCVs that does not exist in other HCV genotypes (Fig. 1B).

There is also a potential for base pair formation between nt 1 of HCV (either guanine or adenine) and nt 17 of miR-122 (uracil) (Fig. 1B). Although we did not investigate this in further detail, the decreased ability of miR-122p6,17G,18C to promote HJ3-5/S1p6m replication (Fig. 3) suggests that it may be important. It is striking, however, that the potential loss of base pairing at HCV nt 1 has less impact than the loss of pairing at nt 4 (compare Fig. 3 and 8C). A model of the seed sequence and 3′ supplementary base pair interactions of miR-122 with the genotype 1a H77S virus, including the recruitment of two miR-122 molecules to the 5′ end of the RNA, is shown in Fig. 9. Although the base pair interactions upstream of the S1 seed match site shown in this model are supported by data presented in this communication, it is important that we were able to achieve only partial rescue of the negative effects of guanine substitutions at nt 2 and 3 of the HCV genome by cotransfection of miR-122 mutants with potentially complementary substitutions at nt 15 and 16 (Fig. 5A and D and 8C). We have no explanation for why this was not observed by Machlin et al. (20), as we encountered this issue with HCV RNAs containing either the genotype 1a or genotype 2a 5′UTR (Fig. 5A and D). mfold predictions suggest that the lack of complete rescue was not due to aberrant folding of the 5′-terminal HCV sequence (Fig. 5C), although this cannot be ruled out entirely.

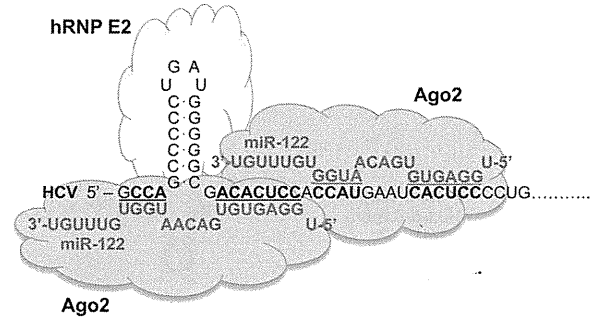


FIG 9 Base pair interactions between miR-122 and the 5′UTR terminal sequences of genotype 1a H77S RNA demonstrated by mutational studies. The model shown includes two distinct Ago2 molecules recruited by miR-122 molecules bound to the S1 and S2 seed match sequences. PCBP2 (hRNP E2) is shown bound to stem-loop 1 as described by Fukushi et al. (10). Interactions of miR-122 with the 5′ 30 nt of the HCV sequence are likely to be more complex than that shown here, since complementary substitutions at nt 2 and 3 of the HCV genome fail to rescue Ago2 recruitment by miR-122p6,15C,16C, targeting the S1 seed match site, and only partially rescue the ability of miR-122p6,15C,16C to promote HCV RNA accumulation in transfected cells.

One possibility, mentioned above, is that the native cytosines are required for recognition by the replicase complex. However, the residual defect in replication of the HJ3-5/GLuc2A-G2,G3 mutant cotransfected with miR-122 containing complementary 15C and 16C substitutions was overcome to a significant extent by an adenine substitution at nt 4 of HCV that is predicted to extend the interaction of miR-122 with nt 2 and 3 of the HCV RNA by an additional base pair (Fig. 8C and D). This suggests that the lack of complete rescue of the 2G,3G mutants may be due to a failure to recreate the native interactions of miR-122 with 5′ HCV RNA upstream of the S1 seed match site rather than a defect in replicase recognition of HCV RNA. This notion is reinforced by the failure of the complementary mutants to stabilize the viral RNA, as shown in Fig. 7A, or to efficiently recruit Ago2, as indicated in the Ago2-RNA co-IP experiment shown in Fig. 7D (left panel). Thus, the interactions of miR-122 with HCV RNA upstream of the S1 seed match site are likely to be more complex than those shown in Fig. 9. It is notable that SHAPE was not able to map the effect of miR-122 on RNA structure upstream of S1 (22), and it is possible that there are several alternative structures, only one of which is shown in Fig. 9. Several conserved cytosines in nt 6 to 10 are predicted to contribute to a stable stem-loop structure in the 5′UTR (SL-1 in Fig. 1B) but, alternatively, could pair with G15 and G16 of miR-122. However, this stem-loop has been suggested to bind poly(rC) binding protein 2 (PCBP2; also known as hRNP E2) (Fig. 9) and to be required for HCV replication (10, 29). Thus, although the data we present here provide a more detailed view of the interaction of miR-122 with HCV RNA than that available previously, it is clear that additional studies will be needed to resolve the structure(s) of the complex formed by miR-122 at the extreme 5′ end of the viral RNA.

## ACKNOWLEDGMENTS

This work was supported in part by grants from the National Institutes of Health (RO1-AI095690 and P20-CA150343) and the University Cancer Research Fund.

## REFERENCES

1. Bartel DP. 2009. MicroRNAs: target recognition and regulatory functions. Cell 136:215–233.

2. **Chang J, et al.** 2004. miR-122, a mammalian liver-specific microRNA, is processed from hcr mRNA and may downregulate the high affinity cationic amino acid transporter CAT-1. RNA Biol. 1:106–113.
3. **Chenna R, et al.** 2003. Multiple sequence alignment with the Clustal series of programs. Nucleic Acids Res. 31:3497–3500.
4. **Combet C, et al.** 2007. euHCVdb: the European hepatitis C virus database. Nucleic Acids Res. 35:D363–D366.
5. **Crooks GE, Hon G, Chandonia JM, Brenner SE.** 2004. WebLogo: a sequence logo generator. Genome Res. 14:1188–1190.
6. **Davis GL, Alter MJ, El-Serag H, Poynard T, Jennings LW.** 2010. Aging of hepatitis C virus (HCV)-infected persons in the United States: a multiple cohort model of HCV prevalence and disease progression. Gastroenterology 138:513–521.
7. **Edgar RC.** 2004. MUSCLE: multiple sequence alignment with high accuracy and high throughput. Nucleic Acids Res. 32:1792–1797.
8. **Fabian MR, Sonenberg N, Filipowicz W.** 2010. Regulation of mRNA translation and stability by microRNAs. Annu. Rev. Biochem. 79:351–379.
9. **Friebe P, Lohmann V, Krieger N, Bartenschlager R.** 2001. Sequences in the 5′ nontranslated region of hepatitis C virus required for RNA replication. J. Virol. 75:12047–12057.
10. **Fukushi S, et al.** 2001. Interaction of poly(rC)-binding protein 2 with the 5′-terminal stem loop of the hepatitis C-virus genome. Virus Res. 73:67–79.
11. **Galtier N, Gouy M, Gautier C.** 1996. SEAVIEW and PHYLO_WIN: two graphic tools for sequence alignment and molecular phylogeny. Comput. Appl. Biosci. 12:543–548.
12. **Grimson A, et al.** 2007. MicroRNA targeting specificity in mammals: determinants beyond seed pairing. Mol. Cell 27:91–105.
13. **Hafner M, et al.** 2010. Transcriptome-wide identification of RNA-binding protein and microRNA target sites by PAR-CLIP. Cell 141:129–141.
14. **Henke JI, et al.** 2008. microRNA-122 stimulates translation of hepatitis C virus RNA. EMBO J. 27:3300–3310.
15. **Jangra RK, Yi M, Lemon SM.** 2010. miR-122 regulation of hepatitis C virus translation and infectious virus production. J. Virol. 84:6615–6625.
16. **Jopling CL, Schutz S, Sarnow P.** 2008. Position-dependent function for a tandem microRNA miR-122-binding site located in the hepatitis C virus RNA genome. Cell Host Microbe 4:77–85.
17. **Jopling CL, Yi M, Lancaster AM, Lemon SM, Sarnow P.** 2005. Modulation of hepatitis C virus RNA abundance by a liver-specific microRNA. Science 309:1577–1581.
18. **Lemon SM, Walker C, Alter MJ, Yi M.** 2007. Hepatitis C viruses, p 1253–1304. *In* Knipe DM, et al (ed), Fields virology, 5th ed. Lippincott Williams & Wilkins, Philadelphia, PA.
19. **Ma Y, Yates J, Liang Y, Lemon SM, Yi M.** 2008. NS3 helicase domains involved in infectious intracellular hepatitis C virus particle assembly. J. Virol. 82:7624–7639.
20. **Machlin ES, Sarnow P, Sagan SM.** 2011. Masking the 5′ terminal nucleotides of the hepatitis C virus genome by an unconventional microRNA-target RNA complex. Proc. Natl. Acad. Sci. U. S. A. 108:3193–3198.
21. **O'Carroll D, et al.** 2007. A Slicer-independent role for Argonaute 2 in hematopoiesis and the microRNA pathway. Genes Dev. 21:1999–2004.
22. **Pang PS, et al.** 2012. Structural map of a microRNA-122: hepatitis C virus complex. J. Virol. 86:1250–1254.
23. **Perz JF, Armstrong GL, Farrington LA, Hutin YJ, Bell BP.** 2006. The contributions of hepatitis B virus and hepatitis C virus infections to cirrhosis and primary liver cancer worldwide. J. Hepatol. 45:529–538.
24. **Roberts AP, Lewis AP, Jopling CL.** 2011. miR-122 activates hepatitis C virus translation by a specialized mechanism requiring particular RNA components. Nucleic Acids Res. 39:7716–7729.
25. **Shimakami T, et al.** 2011. Protease inhibitor-resistant hepatitis C virus mutants with reduced fitness from impaired production of infectious virus. Gastroenterology 140:667–675.
26. **Shimakami T, et al.** 2012. Stabilization of hepatitis C RNA by an Ago2-miR-122 complex. Proc. Natl. Acad. Sci. U. S. A. 109:941–946.
27. **Simmonds P, et al.** 2005. Consensus proposals for a unified system of nomenclature of hepatitis C virus genotypes. Hepatology 42:962–973.
28. **Villanueva RA, et al.** 2010. miR-122 does not modulate the elongation phase of hepatitis C virus RNA synthesis in isolated replicase complexes. Antiviral Res. 88:119–123.
29. **Wang L, Jeng KS, Lai MM.** 2011. Poly(C)-binding protein 2 interacts with sequences required for viral replication in the hepatitis C virus (HCV) 5′ untranslated region and directs HCV RNA replication through circularizing the viral genome. J. Virol. 85:7954–7964.
30. **Yi M, Villanueva RA, Thomas DL, Wakita T, Lemon SM.** 2006. Production of infectious genotype 1a hepatitis C virus (Hutchinson strain) in cultured human hepatoma cells. Proc. Natl. Acad. Sci. U. S. A. 103:2310–2315.

# Stabilization of hepatitis C virus RNA by an Ago2–miR-122 complex

Tetsuro Shimakami[a,1], Daisuke Yamane[a,1], Rohit K. Jangra[a,1,2], Brian J. Kempf[b], Carolyn Spaniel[a], David J. Barton[b], and Stanley M. Lemon[a,3]

[a]Lineberger Comprehensive Cancer Center and Division of Infectious Diseases, Department of Medicine, University of North Carolina at Chapel Hill, Chapel Hill, NC 27599-7292; and [b]Department of Microbiology, University of Colorado School of Medicine, Aurora, CO 80045

Edited* by Charles M. Rice, The Rockefeller University, New York, NY, and approved December 5, 2011 (received for review July 27, 2011)

**MicroRNAs (miRNAs) are small noncoding RNAs that regulate eukaryotic gene expression by binding to regions of imperfect complementarity in mRNAs, typically in the 3′ UTR, recruiting an Argonaute (Ago) protein complex that usually results in translational repression or destabilization of the target RNA. The translation and decay of mRNAs are closely linked, competing processes, and whether the miRNA-induced silencing complex (RISC) acts primarily to reduce translation or stability of the mRNA remains controversial. miR-122 is an abundant, liver-specific miRNA that is an unusual host factor for hepatitis C virus (HCV), an important cause of liver disease in humans. Prior studies show that it binds the 5′ UTR of the messenger-sense HCV RNA genome, stimulating translation and promoting genome replication by an unknown mechanism. Here we show that miR-122 binds HCV RNA in association with Ago2 and that this slows decay of the viral genome in infected cells. The stabilizing action of miR-122 does not require the viral RNA to be translationally active nor engaged in replication, and can be functionally substituted by a nonmethylated 5′ cap. Our data demonstrate that a RISC-like complex mediates the stability of HCV RNA and suggest that Ago2 and miR-122 act coordinately to protect the viral genome from 5′ exonuclease activity of the host mRNA decay machinery. miR-122 thus acts in an unconventional fashion to stabilize HCV RNA and slow its decay, expanding the repertoire of mechanisms by which miRNAs modulate gene expression.**

RNA decay | viral host factor

MicroRNAs (miRNAs) typically regulate eukaryotic gene expression by binding to regions of imperfect complementarity in the 3′ UTR of mRNAs, recruiting an Argonaute (Ago) protein complex that results in translational repression or destabilization of the target RNA (1). Although miRNAs regulate a majority of genes, an unresolved question is whether the miRNA-induced silencing complex (RISC) acts primarily to reduce translation or enhance decay of the mRNA, two closely linked, competing processes (2–4). miR-122 is an abundant, liver-specific miRNA, comprising >50% of mature miRNAs in human hepatocytes and regulating the expression of numerous hepatic genes, including those involved in fatty acid and cholesterol metabolism (5, 6). It is also a very unusual host factor required for replication of hepatitis C virus (HCV), an important cause of liver disease in humans (7, 8). Prior studies show that miR-122 binds the 5′ UTR of the positive-strand HCV RNA genome (7, 9), stimulating viral protein expression and promoting viral replication by a poorly understood mechanism (10, 11).

Although miR-122 does not directly stimulate HCV RNA synthesis (12, 13), its ability to promote genome amplification is independent of its regulation of hepatic metabolism (12) and requires the binding of its "seed sequence" (nucleotides 2–8) to two conserved sites (S1 and S2) in the viral 5′ UTR (7, 9). Additional "supplementary" base-pairing between miR-122 and HCV RNA sequences upstream of S1 and S2 has also been recognized recently and shown to be essential for promotion of genome amplification (14, 15). The miR-122 binding sites are near the 5′ end of the RNA and immediately upstream of an internal ribosome entry site (IRES) that has high affinity for the 40S ribosome subunit (16). The unusual ability of miR-122 to stimulate viral protein translation (10, 11) is dependent on where it binds, because miR-122 suppresses expression of capped reporter mRNAs that contain the HCV target sequence in the 3′ UTR (9). Translation enhancement only partially explains the role of miR-122 in the HCV life cycle, however, because mutant viral RNAs that are deficient in miR-122 binding are far more handicapped in their ability to replicate than viral RNAs with mutations in the IRES that result in quantitatively comparable defects in translation (11).

Although there has been speculation that miR-122 might promote genome amplification and viral protein expression by physically stabilizing HCV RNA (14, 17), previous experimental results suggest this is not the case and that miR-122 does not enhance RNA stability (7, 10). Here we present a contrasting view and show that binding of miR-122 to the 5′ terminus of HCV RNA in association with Ago2 significantly slows decay of the viral RNA genome in infected cells. miR-122 thus acts in an unconventional fashion to stabilize HCV RNA, expanding the repertoire of mechanisms by which miRNAs modulate gene expression.

## Results

We studied how miR-122 influences the stability of synthetic HCV RNA transfected into human hepatoma cells. Northern blots demonstrated significant increases in the abundance of a replication-defective viral RNA (H77S/GLuc2A-AAG, that contains a lethal mutation in its RNA polymerase) (Fig. 1*A*) when it was electroporated into cells together with duplex miR-122 (Fig. 1*B*). miR-124, a brain-specific miRNA that does not bind HCV RNA, had no such effect. Conversely, cotransfection of viral RNA with 2′O-methyl-modified (2′OMe) or locked nucleic acid antisense oligoribonucleotides capable of sequestering miR-122 reduced the abundance of HCV RNA at 3, 6, and 9 h after electroporation. These differences were reproducible in multiple experiments and observed with HCV RNAs containing 5′ UTR sequence from either genotype 1 (H77) or genotype 2 (JFH1) virus. We estimated the rate of viral RNA decay by PhosphorImager analysis of Northern blots, normalizing HCV RNA abundance (HCV RNA/actin mRNA) to that present at 3 h after electroporation to compare rates of

Author contributions: T.S., D.Y., R.K.J., B.J.K., C.S., D.J.B., and S.M.L. designed research; T.S., D.Y., R.K.J., C.S., and B.J.K. performed research; T.S., D.Y., R.K.J., B.J.K., C.S., D.J.B., and S.M.L. analyzed data; and T.S., D.Y., R.K.J., D.J.B., and S.M.L. wrote the paper.

The authors declare no conflict of interest.

*This Direct Submission article had a prearranged editor.

[1]T.S., D.Y., and R.K.J. contributed equally to this work.

[2]Present address: Department of Microbiology, Mount Sinai School of Medicine, New York, NY 10029.

[3]To whom correspondence should be addressed. E-mail: smlemon@med.unc.edu.

This article contains supporting information online at www.pnas.org/lookup/suppl/doi:10.1073/pnas.1112263109/-/DCSupplemental.

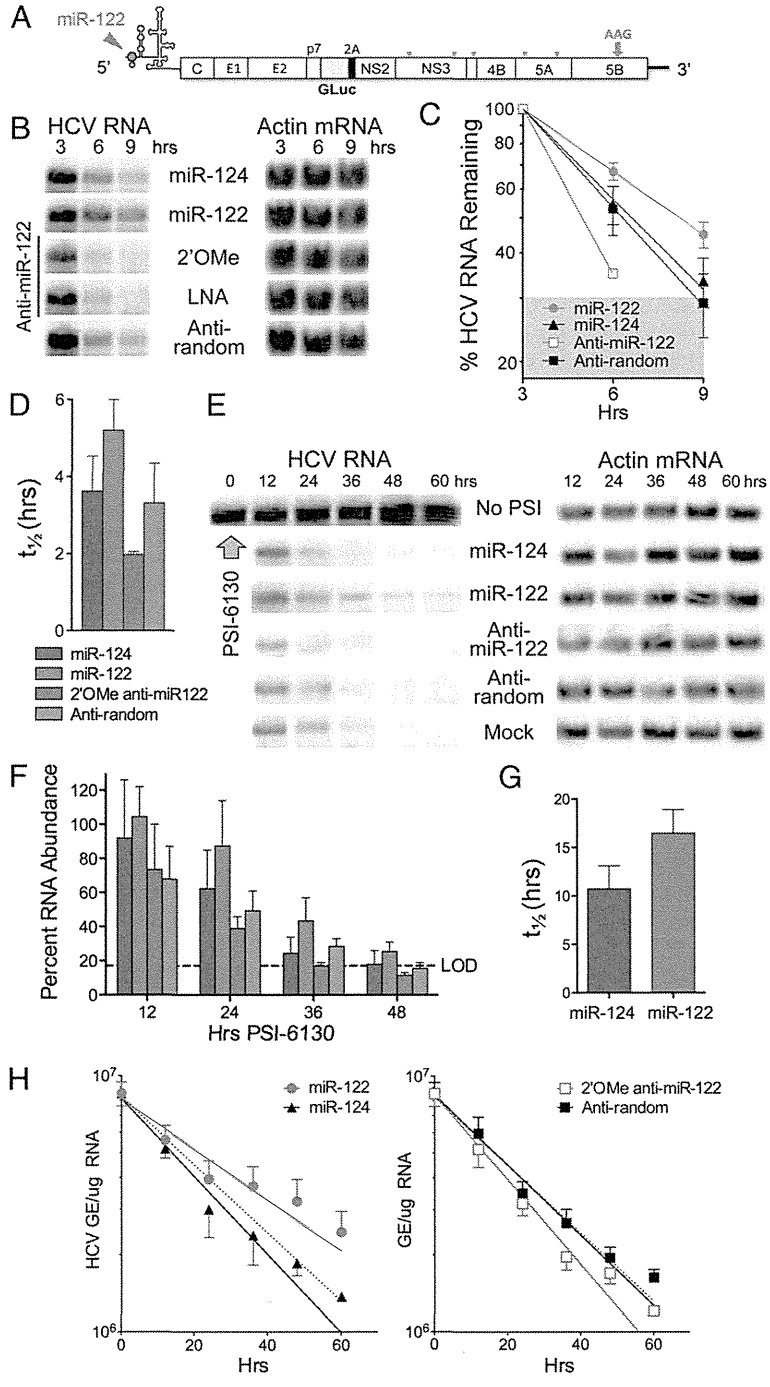


**Fig. 1.** miR-122 stabilizes the HCV RNA genome. (*A*) Organization of H77S/GLuc2A-AAG RNA that expresses GLuc as part of the HCV polyprotein (31). The AAG mutation in NS5B ablates genome amplification. The position at which miR-122 binds the 5′ UTR is shown. (*B*) Northern blot of H77S/GLuc2A-AAG and actin RNA (loading control) in Huh-7.5 cells after electroporation of viral RNA together with duplex miRNAs or antisense oligoribonucleotides. (*C*) Quantitation of HCV RNA relative to actin mRNA by phosphorimaging of Northern blots from five independent electroporation experiments. Data shown represent the mean percentage RNA remaining (±SEM) relative to that present at 3 h after electroporation under each condition. Data were fit to a one-phase decay model ($R^2$ = 0.87–0.99). The shaded area represents the approximate limit of detection (LOD; 9 h posttransfection data from anti-miR-122–transfected cells were below the LOD and excluded from analysis). (*D*) Mean HCV RNA $t_{1/2}$ estimated by fitting the Northern blot data to a one-phase decay model, as shown in *C*. Error bars indicate 95% confidence intervals. (*E*) Northern blot of HCV RNA in persistently infected (>3 wk) cells treated with PSI-6130 (10 μM or >10-fold the $EC_{50}$) and transfected with miRNAs or 2′OMe oligoribonucleotides. (*F*) PhosphorImager quantitation of Northern blots in two replicate experiments involving PSI-6130 treatment. Results were normalized to RNA abundance in mock-transfected cells at 12 h. See *D* for the key. (*G*) Mean HCV RNA $t_{1/2}$ ± SD in cells supplemented with miR-122 vs. miR-124 after PSI-6130 treatment, estimated by fitting PhosphorImager data from four independent experiments to a one-phase decay model. $P$ = 0.007 by two-sided paired $t$ test. (*H*) qRT-PCR determination of HCV RNA decay in infected cells treated with PSI-6130 and supplemented with miRNAs and antisense oligoribonucleotides as in *E*. Data are from three replicate infected cultures, and represent HCV genome equivalents (GE) per μg total RNA ± SD (*left*) HCV RNA in cells supplemented with miR-122 or miR-124. Data were fit to a one-phase decay model ($R^2$ = 0.86–0.95): HCV RNA $t_{1/2}$ =30.3 h for miR-122 vs. 19.8 h for miR-124 ($P$ = 0.018). *Right*: Cells treated with 2′-OMe anti-miR-122 or anti-random ($R^2$ = 0.95–0.96): $t_{1/2}$ =18.2 h for anti-miR-122 vs. 21.9 h for anti-random ($P$ = 0.023). The dashed line in both panels represents the one-phase decay curve in mock-treated cells.

decay between 3 and 9 h under different conditions (Fig. 1*C*). This allowed for recovery of the cells after electroporation, and when the data were fit to a one-phase decay model, indicated that the half-life ($t_{1/2}$) of HCV RNA in cells cotransfected with miR-122 was 5.2 h vs. 3.60 h for cells cotransfected with miR-124 ($P = 0.0035$ by the extra sum-of-squares $F$ test) and 3.3 vs. 2.0 h for cells transfected with anti-random vs. the anti–miR-122 antagomir ($P = 0.0016$) (Fig. 1*D*). Similar differences in rates of decay were observed when HCV RNA was assayed by quantitative RT-PCR (qRT-PCR) (Fig. S1*A*). Differences in RNA decay were matched by differences in viral protein expression (Fig. S1*B*), monitored by measuring *Gaussia* luciferase (GLuc) encoded by sequence inserted into the viral genome (Fig. 1*A*). Taken together, these results indicate that miR-122 positively regulates the stability of transfected HCV RNA. The corresponding increase in protein expression provides a logical explanation for the enhanced HCV translation reported previously (10, 11).

Because transfected RNA is likely to be subject to different decay pathways than replicating viral genomes in infected cells, we determined whether miR-122 also slows degradation of viral RNA in infected cells treated with PSI-6130, a potent and specific nucleoside inhibitor that arrests new viral RNA synthesis (18). Under these conditions, as expected, viral RNA degraded more slowly than after electroporation (compare Fig. 1 *B* and *E*). However, its rate of decay was reduced when miR-122 was transfected simultaneously with PSI-6130 treatment (Fig. 1*E*). When fit to a one-phase decay model, PhosphorImager data from replicate experiments (Fig. 1*F*) indicated a significant difference in the rate constant for HCV RNA decay, $k$ ($k = \ln(2)/t_{1/2}$), in cells supplemented with miR-122 vs. miR-124 ($P = 0.048$ by the extra sum-of-squares $F$ test). The difference in the $t_{1/2}$ was highly significant statistically ($P = 0.007$ by two-sided paired $t$ test) (Fig. 1*G*). Likewise, increases in the decay rate in cells transfected with anti-miR-122 vs. the control anti-random oligonucleotide were also significant ($P = 0.014$ by $F$ test), whereas decay rate constants were similar in cells receiving anti-miR-124, anti-random, or mock treatment ($P > 0.05$). Similar results were observed when miR-122 was transfected into cells 8 h after the addition of PSI-6130, which would allow for any potential delay in suppression of viral RNA synthesis due to the need for phosphorylation of the inhibitor (Fig. S1 *C* and *D*).

In a completely independent set of experiments, we used qRT-PCR to quantify HCV RNA in infected cells treated with PSI-6310. The results suggested a longer $t_{1/2}$ for HCV RNA (≈19 h vs. ≈10 h) in miR-124–treated cells than that determined by Northern analysis. This is likely to reflect the small size of the RNA segment detected in the RT-PCR assay (221 bases vs. the 9.7-kb RNA genome detected in Northern blots) and the inability of the RT-PCR assay to discriminate between intact and partially degraded RNAs. However, we again observed significant differences in HCV RNA decay rates in cells supplemented with miR-122 vs. miR-124, or anti-miR-122 vs. anti-random (Fig. 1*H*). Although the magnitude of this effect is relatively small (not unlike the impact of miRNAs on cellular mRNA translation), these data show collectively that miR-122 reproducibly stabilizes the viral RNA genome in infected cells.

We next determined whether miR-122 could directly stabilize RNA in a cell-free system. For this, we compared poliovirus (PV) RNA and a related RNA (DNVR2) in which the PV 5′ UTR was replaced with the HCV 5′ UTR (Fig. 2*A*). The stabilities of these RNAs have been compared previously in S10 translation mixtures prepared from HeLa cells (19, 20), providing a useful context for these experiments. PV RNA is stabilized in these extracts by poly(rC) binding protein 1 (hnRNP1-E1), which associates with a 5′-terminal cloverleaf RNA structure, and decays more slowly than DNVR2 RNA (20). However, DNVR2 RNA stability was increased and approximated that of PV RNA when duplex miR-122, but not miR-124, was added to S10 reactions before the viral RNA (Fig. 2 *B* and *C*). The stabilization of DNVR2 RNA by miR-122 was reproducible and statistically significant (Fig. 2 legend). In contrast, neither miRNA enhanced stability of PV RNA lacking HCV sequence. Thus, miR-122 directly regulates stability of RNA containing the HCV 5′ UTR and does not accomplish this indirectly by modulating cellular gene expression.

Mutations in S1 and S2 that ablate miR-122 binding are lethal to replication of HCV that has been adapted to growth in cell culture (HJ3-5 virus) (11). Similarly, Northern blots revealed that an HCV mutant defective in miR-122 binding at both sites (S1-S2-p6m; Fig. 3*A*) (11), as well as polymerase function (GDD to GND substitution in NS5B), was not stabilized by miR-122 when transfected into hepatoma cells (Fig. 3*B*, compare lanes 1–3 vs. 4–6). In contrast, the complementary miR-122 mutant (miR-122p6) (Fig. 3*A*) did stabilize S1-S2-p6m RNA (Fig. 3*B*, lanes 1–3 vs. 7–9) but not viral RNA with WT S1 and S2 sequences. The differences in HCV RNA abundance apparent in these blots were reproduced in multiple experiments, statistically significant (Fig. S2*A*), and mirrored by differences in GLuc expressed from these nonreplicating viral RNAs (Fig. S2*B*). Collectively, these data indicate that HCV RNA is physically stabilized as a result of miR-122 binding to its 5′ UTR, a unique action for a miRNA.

Because mRNA translation and decay are closely coupled processes (2), we considered the possibility that miR-122 could stabilize the RNA by promoting its translation. We thus evaluated its ability to slow decay of an RNA containing three consecutive base substitutions in an RNA loop within the HCV IRES [mutant G(266-8)C; Fig. 3*C*]. These base changes eliminate IRES affinity for the 40S ribosome particle and ablate translation (11, 16), even in cells supplemented with miR-122 (Fig. S3*A*). Consistent with the notion that translation and decay are intrinsically linked (2), Northern blots of cells transfected with equivalent amounts of WT and G(266-8)C RNA (both containing an NS5B mutation ablating RNA replication) consistently showed a lower abundance of the G(266-8)C mutant, suggesting that it was less stable than RNA with a WT 5′ UTR (Fig. 3 *D* and *E*). Nonetheless, decay of the translationally

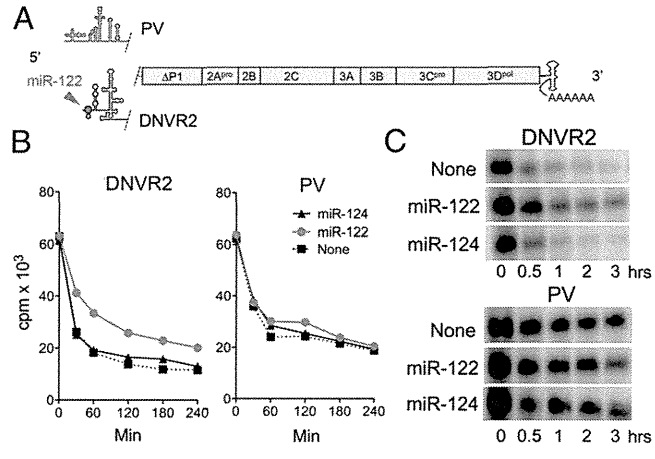


**Fig. 2.** miR-122 stabilizes synthetic RNA containing the HCV 5′ UTR. (*A*) Structure of DNVR2 and PV RNAs (19), which differ only in 5′ UTR sequence. (*B*) miR-122 slows decay of DNVR2 RNA in HeLa S10 lysate. Data shown represent acid-precipitable α-[$^{32}$P]-CTP-labeled RNA in HeLa S10 reaction mixtures (19) containing 1 μM of duplex miRNA. The DNVR2 decay constant in miR-122– vs. miR-124–supplemented mixtures, estimated by fitting the data to a one-phase decay model ($R^2 = 0.972$–$0.989$), differed significantly ($P = 0.002$). (*C*) RNA extracted from HeLa S10 reaction mixtures and fractionated by electrophoresis in 0.8% agarose.